

NASA Technical Memorandum 86771

IN-02  
DATE OVERRIDE  
102787  
P.41

(NASA-TM-86771) TRANSONIC ROTOR TIP DESIGN  
USING NUMERICAL OPTIMIZATION (NASA) 41 p  
Avail: NTIS HC A03/MF A01 CSCL 01A

N87-29431

Unclas

G3/02 0102787

---

# Transonic Rotor Tip Design Using Numerical Optimization

---

Michael E. Tauber and Ronald G. Langhi

---

LIBRARY COPY

OCT 29 1985

LANGLEY RESEARCH CENTER  
LIBRARY, NASA  
HAMPTON, VIRGINIA

October 1985



National Aeronautics and  
Space Administration

Date for general release October 1987

---

# Transonic Rotor Tip Design Using Numerical Optimization

---

Michael E. Tauber, Ames Research Center, Moffett Field, California  
Ronald G. Langhi, Informatics General Corporation, Palo Alto, California

October 1985



National Aeronautics and  
Space Administration

**Ames Research Center**  
Moffett Field, California 94035

# TRANSONIC ROTOR TIP DESIGN USING NUMERICAL OPTIMIZATION

Michael E. Tauber and Ronald G. Langhi\*

Ames Research Center

## SUMMARY

The aerodynamic design procedure for a new blade tip suitable for operation at transonic tip speeds is illustrated. For the first time, three-dimensional numerical optimization was applied to rotor tip design, using the recent derivative of the ROT22 code, program R22OPT. Program R22OPT utilized an efficient quasi-Newton optimization algorithm. Multiple design objectives were specified. The delocalization of the shock wave was to be eliminated in forward flight for an advance ratio of 0.41 and a tip Mach number of 0.92 at  $\psi = 90^\circ$ . Simultaneously, it was sought to reduce torque requirements while maintaining effective restoring pitching moments. Only the outer 10% of the blade span was modified; the blade area was not to be reduced by more than 3%. The goal was to combine the advantages of both swept-back and swept-forward blade tips (configurations which had been studied previously). A planform that featured inboard sweepback was combined with a swept-forward tip using a taper ratio of 0.5. Initially, the ROT22 code was used to find by trial and error a planform geometry which met the design goals. This configuration had an inboard section with a leading edge sweep of  $20^\circ$  and a tip section swept forward at  $25^\circ$ ; in addition, the airfoils were modified. With this tip shape as a starting point, program R22OPT was used to improve the planform and airfoil section design. Significant improvements, which met all design objectives, were achieved in 2.5 CPU hours on a CRAY X-MP computer. The optimized tip has an inboard sweepback of  $19.7^\circ$ , a tip swept forward at  $34.1^\circ$ , 50% of taper, and modified airfoil sections.

## INTRODUCTION

The inevitable increase in forward flight speeds of conventional helicopters has resulted in higher rotor tip Mach numbers. However, forward flight speed can be limited by the increased wave drag caused by the presence of large regions of supersonic flow on the outer part of the advancing blade. Another undesirable feature resulting from this supersonic flow can be a large increase in the noise emanating from the rotor blade. Strong shock waves forming on the blade tip can propagate efficiently into the far field, producing intense low-frequency noise. To lessen these drag and noise increases, rotor tips designed to reduce shock strengths have been extensively studied (ref. 1-6). (In fact, most new high-speed helicopters have swept-back rotor tips.)

---

\*Informatics General Corp.

Although swept-back rotor tips have been successfully used in recent years, such a tip configuration is generally not optimum. Since the tip is normal to the oncoming free stream in the second quadrant, the torque requirements can exceed those for a rectangular blade in that position (refs. 6 and 7). Reference 6 theoretically shows that a swept-forward tip offers both torque and acoustic advantages over a swept back one. However, swept-forward lifting surfaces have a well-known tendency toward angle-of-attack divergence instability which can produce severe vibration (although it may be possible to restrain the divergence by using anisotropic composite materials). To avoid the structural and dynamic problems of the swept-forward tip, it was decided to investigate tip shapes which would be aerodynamically stable, yet combine the best features of both forward and aft sweep. The theoretical study was made using the ROT22 transonic, full-potential, three-dimensional rotor code and its recent derivative, R22OPT, which is suitable for optimization.

The next section briefly discusses the development of ROT22 and R22OPT, including the main features and the simplifying assumptions of both codes. A description of the application of the codes to the design of a new, multiply-swept blade tip follows. The modification of both the tip planform and the airfoil sections in the tip region will be demonstrated on a hypothetical modern lifting rotor blade with an initially rectangular planform and a supercritical airfoil.

## BRIEF DESCRIPTION OF ANALYSIS

### Program ROT22

The earliest codes developed for calculating the high-speed flow over a rotor blade solved the transonic small disturbance equation (refs. 8-10). The ROT22 code represented the first solution of the full potential equation for the flow over a rotary wing. Since ROT22 has been previously documented (refs. 11 and 12), its main features and assumptions will be only briefly reviewed here.

Beyond the assumptions inherent in the potential equation, the simplifications embodied in the model are: a single-blade analysis, a simplified mathematical treatment of the vortex sheet behind the blade, an approximate wake-induced inflow, and a quasi-steady flow field. Because the full-potential equation and the exact tangency boundary condition are used, subsonic and transonic flow over thick airfoils with blunt leading edges and at angle of attack can be modeled realistically. There are no inherent geometric limitations; airfoil section and chord can be varied, together with pitch angle, angle of attack, twist, and flapping angle. The code is inviscid and contains a relatively simple, curved, kinematically determined near-wake. Wake-induced inflow can be approximately modeled by judicious placement of vortices in the flow field. Provisions exist for two straight vortices. Thus, the tip vortex shed from a preceding blade can be approximately simulated. The strength of the vortices is determined from the circulation on the blade and the vortex core size is based on the correlation of reference 13.

The governing equations (potential and energy) are rendered quasi-steady by setting all the time derivatives of the perturbation potential equal to zero; however, the effects of rotation are maintained with the quasi-steady assumption. Although the time history is removed from the solution for forward flight, the equations and the boundary conditions retain a timelike dependence by being a function of rotor position. The assumption of quasi-steady flow permits computing the flow field about the blade at one azimuth angle. This speeds the computation by nearly two orders of magnitude in comparison with a fully unsteady calculation. (In an unsteady computation, the azimuth angle can be increased only a fraction of a degree between time steps as the blade advances into the airstream (ref. 14).) The effect of the quasi-steady assumption was assessed in reference 15. Here, computed surface pressure distributions around the entire rotor disk were compared with measured values near the tip on both straight- and swept-tip model rotors to advance ratios of 0.45 and to a maximum tip Mach number of 0.91. The agreement between calculated and measured pressures was found to be good. In fact, at the important 90° blade azimuth position, the theoretical and experimental values compared very well to an advance ratio of 0.5, corresponding to a tip Mach number of 0.94.

While many sources of helicopter noise have been identified (ref. 16), impulsive noise was found to dominate the noise spectrum at high speed (ref. 17). In reference 17, Schmitz and Yu explained the cause of high-speed impulsive noise as the propagation of shock waves occurring on the advancing blade into the acoustic far-field, a mechanism which they labeled "delocalization." Thus, the accurate prediction of velocities in the vicinity of and beyond the blade tip is critical to the determination of transonic noise propagation into the acoustic far-field. It had been shown previously (eq. (1), ref. 6) that rotor-generated noise caused by the formation of shock waves on the blade propagated most effectively when the blade was at the 90° azimuth position because the sonic surface was closest to the blade tip. The unperturbed sonic surface is located at

$$S = \left( \frac{1}{M_{rot}^2} - \mu^2 \cos^2 \psi \right)^{1/2} - \mu \sin \psi \quad (1)$$

where  $S$  is measured from the center of rotation,  $M_{rot}$  is the rotational Mach number,  $\mu$  is the advance ratio, and  $\psi$  is the azimuth angle. ROT22-computed and experimentally measured velocities were extensively compared in this part of the flow field (ref. 18). In the experiment, laser velocimeter measurements were made of the three orthogonal velocity components in the neighborhood of the tip of a nonlifting, hovering model rotor at tip Mach numbers from 0.85 to 0.95. The measurements were made in three vertical planes, one located two-thirds of a blade chord inboard of the tip, one at the tip, and one at the unperturbed sonic circle. Each extended one chord above the blade. The ROT22-calculated velocities agreed very well with the LV measurements, as did the prediction of the strength and position of the shock waves. Since the angle of incidence of the advancing blade tip in the vicinity of 90° is usually small, the ROT22 code can be used with the reasonable confidence to predict the important tip-region flow field. The same utility extends to R22OPT which is derived from ROT22.

## Program R22OPT

Linking ROT22 with minimization algorithm QNMDIF has resulted in program R22OPT, which retains all of the capabilities of ROT22 but has been drastically reorganized to meet the requirements of numerical optimization. These requirements include evaluating multiple design points in the same run (typically the fully advancing and fully retreating blade positions), matching prescribed pressure or Mach number distributions at arbitrary computational span stations, perturbing the blade sections or planform (or both), and computing the flow field for each perturbation as efficiently as possible.

### Quasi-Newton Optimization Method

QNMDIF is a general-purpose, unconstrained, quasi-Newton minimization program using finite difference approximations to first derivatives. The quasi-Newton algorithm seeks the minimum of a quadratic model to an objective function of  $N$  variables by stepping in a descent direction derived from gradient information and from a matrix that approximates second derivatives. The second derivative information improves as optimization proceeds. If the objective were truly quadratic, the quasi-Newton method theoretically would locate the minimum in  $N$  steps. Any desired constraints must be included in the objective as penalty functions or be imposed implicitly by the construction of the problem.

Typically, the accuracy of the flow calculations is far less than the available machine precision. The current implementation of QNMDIF is effective even with objective functions having less than full machine precision. It uses a scheme to estimate appropriate finite differencing intervals, which contributes to successful optimization of nonanalytic functions such as those being evaluated (refs. 19 and 20).

### Design by Optimization

The basic concept of aerodynamic design by optimization is well documented (refs. 20 and 21): specify target aerodynamic characteristics and seek to match them by reshaping the lifting surface geometry. The difference between the computed flow quantities and the collection of targets constitutes the objective function to be minimized. Each evaluation of this function involves at least one flow field computation, which is itself an iterative process. Reliable optimization needs a minimum of four or five significant digits in the objective. R22OPT monitors the precision of the objective by evaluating and printing it at every iteration of each flow solution. The precision required by the optimizer typically demands a higher level of flow convergence than is normally considered adequate for ROT22. A maximum correction criterion on the order of  $1.E-07$  is usually needed for optimization.

Objective function evaluations dominate the cost of a run, and the number of evaluations required is directly proportional to the number of design variables

used. R22OPT accepts as few as one input station per planform discontinuity in defining the blade geometry. Since section modifications are applied at the input stations, the sparse blade definition leads to an economy of design variables.

High convergence criteria and multiple function evaluations of this type place a heavy load on a computer's central processing unit (CPU). Even with the well-vectorized flow solver common to both R22OPT and ROT22, one flow solution from start using a  $120 \times 16 \times 48$  mesh takes about 250 CPU seconds for 400 iterations on a CRAY X-MP. Both R22OPT and QNMDIF provide for starting from existing flow solutions and optimization data, respectively. This allows a run to be interrupted and resumed without a loss of information. The flow solutions within an optimization run use a neighboring flow field as a starting guess, with a limit of 200 iterations for any one solution imposed after the first function evaluation. Many of the evaluations require far fewer iterations.

#### BASIC CONFIGURATION AND DESIRED MODIFICATIONS

This study postulates a hypothetical modern rotor blade which is representative of those used on high-speed helicopters. The blade was assumed to have the following characteristics (ref. 6): an aspect ratio of about 10, a linear twist variation from hub to tip of  $-10^\circ$ , and an NLR-1 supercritical airfoil having a maximum 8.7% thickness-to-chord ratio. A rotational tip Mach number of 0.65 (725 ft/sec) and an advance ratio of 0.41 were used; the corresponding forward flight speed was 90.6 m/sec (176 knots). The maximum tip Mach number, at  $\psi = 90^\circ$ , was about 0.92. The cyclic pitch angle,  $\theta_c$ , of the advancing blade was described by

$$\theta_c = 10.7 - 11.2 \sin \psi \quad (2)$$

and was  $-0.5^\circ$  at  $\psi = 90^\circ$  and  $1^\circ$  at both  $\psi = 60^\circ$  and  $120^\circ$ . The conditions were considered to be representative of typical high-speed flight. This geometrically simple blade with a rectangular tip exhibited strong delocalization at these flight conditions.

Only the outer 10% of the blade (0.977 chord length) was modified (ref. 6). The amount of tip taper was constrained so that the decrease in total blade area was less than 3%. For structural reasons, it was desirable to decrease the airfoil thickness-to-chord ratio no more than 20% so that the value at the blade tip would not be less than 7%. The following performance improvements over a rectangular blade were stipulated for the azimuth angle range from  $60^\circ$  to  $120^\circ$ : (1) delocalization was to be eliminated, (2) the torque requirements were to be reduced, (3) the restoring pitching moments were to be at least as large, and (4) the thrust coefficients were not to be decreased significantly. The ROT22 code was used to find, by trial-and-error, an improved tip configuration. Once the feasibility of meeting the design objectives had been proven, R22OPT was used to achieve additional performance improvements.

## Planform Modifications

Two types of tip-planform modifications were investigated. These consisted of taper and various combinations of fore and aft sweep. Initially, the tip taper was based on the results of a previous design study (ref. 6) which had established the effectiveness of using 50% taper on the outer 10% of the blade in reducing or eliminating delocalization. The resulting 2.8% blade area reduction was within the desired 3% limit. When the R22OPT code was used, tip taper was made a design variable; however, the total area reduction was constrained to 3%. The sweep modifications were applied after dividing the outer 10% of the blade into two equal segments of about one-half chord length each. The two segments were then swept at different angles. Sweeping the inboard half of the tip forward and the outboard half aft moved the aerodynamic center of the tip forward of that of the remainder of the blade, and produced the same undesirable pitching moment behavior characteristic of the entirely swept forward tip (ref. 6). It was decided, therefore, to concentrate on using sweepback inboard and to sweep the tip forward. The leading edge sweep angles which were used in ROT22 computations ranged from 10° to 25° for the inboard part, and from -15% to -25% for the outboard part. When R22OPT was used, the leading edge sweep angles of both portions of the tip were made design variables.

## Airfoil Modifications

The contours of the NLR-1 airfoil were modified at selected spanwise blade stations on the outer 10% of the blade by adding geometric shape functions to the original ordinates of the airfoil. The shape functions were added linearly to the baseline profile's upper and lower surface to achieve the desired aerodynamic improvements. The surface perturbations were faired linearly to zero at the 90% spanwise blade station.

In the ROT22 code, three types of shape functions were used to modify the airfoil sections in the tip region. These consisted of an exponential, a sine, and a droop function (ref. 22). Combinations of these three functions had previously been used successfully to design proposed two-dimensional (ref. 21) and three-dimensional (ref. 23) rotorcraft lifting surfaces. The exponential function predominantly affects the leading-edge region and is useful either in achieving efficient supercritical flow or in modifying leading-edge pressure gradients to improve stall progression. The sine function is especially useful for weakening shock waves by changing local curvature of the airfoil at selected chordwise locations; it can be used more than once at each section. The droop function, which was added symmetrically to the upper and lower surfaces, produces a vertical displacement of the forward region of the profile; it is useful in controlling leading-edge pressure gradients and in eliminating shocks on the lower surface in the leading-edge region.

In the R22OPT code, airfoil section modifications were made by adding Wagner functions (ref. 24) to the original airfoil's ordinates. The Wagner functions were more practicable when optimization was used since fewer variables were needed to describe the airfoil modifications than if shape functions had been used. In



practice, however, some flexibility was lost. Since the number of design variables had to be limited to control computation time, the Wagner functions were only applied to the upper surface of the blade. Had shape functions been used, for example, the upper and lower leading edge region could have been modified simultaneously with the droop function.

## RESULTS AND DISCUSSION

To illustrate how the codes were used to design a blade tip for more effective and quieter operation at transonic tip speeds, the flow was calculated on the rectangular and modified tip configurations. Since the blades all developed lift, a longitudinal vortex was placed 10% inboard of the tip and one chord below the blade to simulate a vortex shed from a preceding blade. Using a mesh having 120 cells chordwise, 48 spanwise, and 16 vertically resulted in 33 computational planes positioned normal to the blade surface. Nonlinear spanwise grid spacing was used to improve resolution in the tip region; seven of the computational stations were placed on the outer 10% of the blade, with another seven beyond the blade tip. The outermost grid plane was 0.1556 blade radii (about 1.5 chords) beyond the tip. The combination of the 0.41 advance ratio and the rotational tip Mach number of 0.65 resulted in the idealized sonic surface being 0.1285 blade radii from the tip at  $\psi = 90^\circ$  (from eq. (1)). The sonic surface was, therefore, well within the computational domain at the  $90^\circ$  blade azimuth position where delocalization was most likely to occur.

The flow field, and especially delocalization, can be graphically presented by plotting contours of constant Mach numbers from the solutions. Up to 20 contour lines can be shown at chosen Mach numbers, both on the blade surface and off the surface in the plane of the blade. Since any desired contour can be highlighted, the use of a heavy dashed line for the sonic line and dotted ones for the remaining contours permitted easy identification of the extent of delocalization.

First, the flow field on the blade with the previously listed double-cranked tips was calculated using the ROT22 code. In this manner, a tip geometry which met the design objectives was identified. This tip geometry was then used as a starting point for optimization to illustrate how the R22OPT code can be used to improve the initial design.

### Program ROT22 Tip Design

Initially, the flow field about the basic unmodified rectangular blade was calculated using the ROT22 code. At the  $90^\circ$  azimuth position, the cyclic pitch was  $-0.5^\circ$ ; the advance ratio of 0.41 and the rotational tip Mach number of 0.65 resulted in a tip Mach number of about 0.92. Although all calculations were made using the entire blade, for clarity only enlarged views of the tip region flow field will be shown. Contours of constant Mach number on the upper (higher-speed) surface of the

blade and in the plane of the blade are shown in figure 1. The Mach number contours generally began at 0.8 and went to the peak value in 0.05 intervals, although the more critical transonic values were plotted in increments of 0.02.

Impulsive noise occurs when the shock wave terminating the supersonic flow concentrated in the tip region of the advancing blade extends into the far-field, beyond the blade tip. In the blade-attached coordinate system of the present calculation method, delocalization would correspond to an open sonic line. This delocalization is clearly illustrated in figure 1. The heavy dashed contour represents the sonic line. The large size of the supersonic region beyond the tip, which even at its narrowest point is nearly half a blade chord wide, is apparent. The shock forming on the blade propagated into the flow field beyond the tip, perturbing the sonic surface significantly from the location predicted by equation (1). (Note also that about one chord inboard of the tip on the blade surface there are two supersonic zones, separated by a narrow strip of subsonic flow. This flow pattern is a result of the presence of a double shock, an undesirable phenomenon occurring on supercritical airfoils operating at off-design conditions.)

The inviscid coefficients of thrust,  $C_T$ , torque,  $C_Q$ , and pitching moment,  $C_M$ , were calculated for the entire blade at advance angles from  $60^\circ$  to  $120^\circ$ , using the cyclic pitch variation of equation (2). The force and moment coefficients for the rectangular blade will be used as reference values for comparison with those for the blades having modified tips. The results for the rectangular blade are presented in table 1.

The ROT22 code was used to calculate the flow on the entire blade at the  $90^\circ$  azimuth position where delocalization was most likely to occur. The tip taper was fixed at 50% while the sweep of the two portions of the tip section were systematically varied. The values ranged from  $10^\circ$  to  $25^\circ$  sweepback for the inboard part and  $-15^\circ$  to  $-25^\circ$  of (forward) sweep for the tip. Approximately five or six combinations of sweep were investigated in increments of  $5^\circ$ . Each computer run required about one minute of CPU time on the CRAY X-MP. As the sweep angle of the two sections was increased to  $25^\circ$  and  $-25^\circ$  (the largest values considered for each part) delocalization was eliminated. However, a small pocket of high Mach number flow formed aft of the "V" where the two swept sections joined. Since the flow was accelerated as the sweep angles increased, it was decided to reduce the sweepback of the inboard portion to  $20^\circ$ . Although delocalization reoccurred, the supersonic region beyond the tip was only 0.1 of a chord length wide at its most narrow part (fig. 2). However, the peak Mach number on the blade, aft of the V, was still between 1.40 and 1.45, resulting in a very strong shock followed by a weaker one (fig. 3). Although the strong shock was limited to a very small region on the blade, the resultant wave drag raised the torque to that of the rectangular blade. The thrust and pitching moments were nearly the same for both blade configurations. It was therefore, necessary to modify the NLR-1 airfoil sections on the entire tip to try to eliminate delocalization. In addition, the shock strengths had to be reduced to decrease the wave drag responsible for the high torque.

The airfoil modifications were made by applying the previously described exponential, sine, and droop shape functions. The functions were used at each of the

seven stations with the sine function being used twice at all except the tip. The initial choice of coefficients (ref. 23) for the functions was based on previous experience with modifying the NLR-1 airfoil section (ref. 6). Approximately 15 computer runs were made during which the most important of the 74 shape function coefficients were manually varied. The resulting modifications eliminated delocalization (fig. 4) and reduced the torque by over 20%. The thrust and pitching moments were only minimally affected. Not surprisingly, it was necessary to make the airfoil about 10% thinner at the V; this reduced the peak Mach number by almost 0.15. The corresponding shock strengths have also been greatly reduced on both the upper and lower surfaces (fig. 5).

Additional flow calculations were also made over the azimuth arc from 60° to 120°. The present preliminary configuration exhibited no delocalization, required 10% to 20% less torque, and matched the thrust and pitching moment behavior of the rectangular blade. The Mach number contours and pressure distributions for  $\psi = 60^\circ$  and  $\psi = 120^\circ$  are shown in figures 6 and 7, and 8 and 9, respectively. The peak Mach numbers on the blade were 1.35 at  $\psi = 60^\circ$  and 1.30 at  $\psi = 120^\circ$ . Next, the application of optimization will be illustrated in an effort to improve the design further.

#### Program R22OPT Tip Design

Numerical optimization was applied to the 20°/-25° planform of the final hand-modified configuration described above, with the original NLR-1 airfoil section retained. All optimization computations were made at the 90° blade azimuth position. R22OPT was run with 48 computational span stations, such that the V created by the intersection of the cranked portions of the blade was aligned between two stations. This placement was chosen because the steep spanwise velocity gradients existing there cause the flow field calculations to oscillate if a computational station is at or very near the V. Blade section modifications were effected by use of Wagner shape functions, combinations of which resemble airfoil surfaces (refs. 20, 22, and 24).

Optimization began with 15 variables, consisting of the two tip planform sweep angles and the tip chord, and two sets of the first six Wagner functions. The Wagner functions were applied to the airfoil upper surface at the V and the blade tip; the functions were linearly faired to zero at the 90% blade radial station. The object was to reduce the peak Mach numbers in the region from 5% of the span inboard of the tip to 6.7% outboard. Constraints were imposed on the total blade force coefficients of thrust, torque, and pitching moment via penalty functions to achieve the desired aerodynamic characteristics. The tip area was held constant by adjusting the chord at the V as the tip chord varied. The initial optimization step took 2350 CPU seconds on the CRAY X-MP (running under COS 1.13). The resulting Mach number contour plot showed that the sonic zone delocalization had been eliminated. The crank angles had changed to 19.7° and -34.1°, while the tip chord remained essentially unchanged at 50% taper. The force coefficients were acceptable, and the flow computations converged smoothly.

Subsequently, the flow solutions began to oscillate as the forward sweep of the tip section increased further. Because the configuration resulting from the first optimization step provided smooth convergence, it was decided to fix the planform at the angles of  $19.7^\circ$  and  $-34.1^\circ$ , and to concentrate the limited amount of time remaining upon improving the airfoil sections. Eight to twelve Wagner function variables were used to modify the airfoil sections. After 23 additional optimization steps, the design objectives had been met. These final 23 steps required 6800 CPU seconds, bringing the total computing time for the optimization to just over 2.5 CPU hr. (Although the optimization was only done at the  $90^\circ$  blade azimuth position, the 2.5 hr of CPU time should not be considered excessive. A previous design optimization of a two-dimensional rotorcraft airfoil (ref. 21) required a roughly comparable amount of computing time. (Approximately 30 hr of CPU time on a CDC 7600 computer were used. However, the CDC 7600 was an order of magnitude slower than the CRAY X-MP computer used in the present study.)

Next the computed performance characteristics of the optimized ( $19.7^\circ/-34.1^\circ$ ) tip will be discussed and compared with the starting tip shape of  $20^\circ/-25^\circ$  and, finally, with the rectangular blade. The Mach number contours for the  $90^\circ$  advancing blade position are shown in figure 10. Although the peak value is 1.35 (or 0.1 higher than for the  $20^\circ/-25^\circ$  tip), the width of the subsonic region beyond the tip is 50% greater for the optimized tip. The optimized tip also had a 15% greater restoring pitching moment than the  $20^\circ/-25^\circ$  tip. However, the torque was 6% higher, partly since the maximum surface Mach number was higher and partly because the lower leading edge lip shock was still present on the inboard, swept back portion (fig. 11).

The performance of the optimized tip over the remainder of the advancing blade arc was also calculated, although it was not included in the optimization process. The Mach number contours at  $\psi = 60^\circ$  are shown in figure 12. The maximum value is 1.45, or again 0.1 higher than for the starting tip shape. The higher Mach number caused a strong shock to form aft of the V (fig. 13). The strong shock increased the torque requirement by 7% over that for the starting shape; however, the pitching moment improved by 19%. At the  $120^\circ$  blade position, the peak Mach number was again 0.1 higher (see fig. 14) than for the configuration that was used to start the optimization. The shock on the inboard, swept back part was very strong (see fig. 15). However, the torque was only 2.5% higher for the optimized tip, while the pitching moment value improved by 10%.

By comparing the Mach numbers on the optimized configuration (figs. 10, 12, and 14) with those of the starting one (figs. 2, 6, and 8), it can be seen that they are consistently higher, especially aft of the V. The higher Mach numbers resulted from the greater change in direction that the flow on the optimized tip experienced at the V, and is proportional to the included angle of the V. For the optimized tip, the included angle was  $126^\circ$ , compared to  $135^\circ$  for the tip shape at the start of optimization. Had viscous effects been present in the codes, the optimized configuration might have had a shallower included angle between the two tip portions. Otherwise, the strong shocks would likely induce boundary layer separation which would have resulted in a large increase in drag and torque.

Finally, the torques and pitching moments were compared for the optimized configuration ( $19^\circ/-34.1^\circ$ ) and the start-of-optimization shape ( $20^\circ/-25^\circ$ ) with two previously studied tip shapes (ref. 6). The tip shapes of reference 6 both had the same 50% taper; one had  $30^\circ$  leading edge sweepback, while the other had  $20^\circ$  of leading edge forward sweep. All results were normalized by those for a rectangular blade, therefore including the rectangular tip in the comparison also. However, a more important reason for presenting normalized values is to suppress viscous effects which are important in determining torques. The normalized torque coefficients for blades with the four tip configurations are shown in figure 16 for advancing blade angles from  $60^\circ$  to  $120^\circ$ . Note that the  $20^\circ$  swept forward tip had the lowest torque and the  $30^\circ$  swept back tip the highest from  $\psi = 70^\circ$  to  $120^\circ$ . The double-cranked tips, however, always required less torque than the rectangular blade, with the  $20^\circ/-25^\circ$  being the lower one. The optimized tip's torque was 7% below the rectangular blade at  $\psi = 60^\circ$ , 16% below at  $90^\circ$ , and 6% less at  $120^\circ$ . It was in the restoring pitching moment comparison that the optimized tip fared best, however, while the disadvantage of the  $20^\circ$  swept forward tip was most obvious (fig. 17). The pitching moments of the blade with the optimum tip were 36% higher than the rectangular configuration at  $\psi = 60^\circ$ , 10% higher at  $90^\circ$ , and 7% higher at  $120^\circ$ . These values were from 10% to 20% higher than the pitching moments of the  $20^\circ/-25^\circ$  tip; therefore, the design objectives had been met. The blade area reduction of 2.8% was within the 3% limit that was specified. The thinnest airfoil section was at the tip (see fig. 15) and had a maximum thickness-to-chord ratio of 7.04%, corresponding to a decrease of 19%. (Since the thrust coefficients of the modified blade differed from those of the rectangular blade by only a few percent over the advancing blade arc from  $60^\circ$  to  $120^\circ$ , they were not shown.)

#### CONCLUDING REMARKS

Three-dimensional numerical optimization was used for the first time in aerodynamic design of a high-speed rotor tip. A tip planform geometry consisting of a swept-back section and a forward-swept tip, combined with 50% taper, meets all the design objectives. Twenty-four computer optimization cycles were required using from 8 to 15 design variables. The 2.5 CPU hr of computing time on a CRAY X-MP was considered moderate for a three-dimensional aerodynamic optimization calculation.

When comparing the improvements in the design achieved through optimization, several limitations should be kept in mind. Since numerical optimization in three-dimensional flow is not a fully automated process, the dominant limitation here was time, both in man-hours and in active CPU time. For instance, time constraints limited the application of optimization to the  $90^\circ$  blade azimuth position only. Had other blade positions been included in the study, such as  $60^\circ$ ,  $120^\circ$ , and  $270^\circ$ , the final configuration could have been altered substantially. Also, had more time been available, the Wagner functions could have been applied to the lower surfaces of the airfoil sections, instead of only the upper surfaces. Thus, the wave drag and resultant torque could have been further reduced. Therefore, the optimized configuration should not necessarily be considered an optimum design, although all the

design objectives have been met. Rather, the results illustrated here should be considered an example of the successful application of the R22OPT code to the computerized aerodynamic design process.

## REFERENCES

1. Tauber, M. E.: Analytic Investigation of Advancing Blade Drag Reduction by Tip Modifications. 34th Annual National Forum of the American Helicopter Society, Washington, D.C., May 15-17, 1978. Paper no. 78-1, pp. 78-1-1 to 78-1-9.
2. Stroub, R. H.: Full-Scale Wind Tunnel Test of a Modern Helicopter Main Rotor- Investigation of Tip Mach Number Effects and Comparisons of Four Tip Shapes. 34th Annual Forum of the American Helicopter Society, Washington, D.C., May 15-17, 1978. Paper no. 78-3, pp. 78-3-1 to 78-3-6.
3. Shenoy, K. R.: A Semiempirical High-Speed Rotor Noise Prediction Technique. 38th Annual Forum of the American Helicopter Society, Anaheim, Calif., May 4-7, 1982, pp. 508-516.
4. McVeigh, M. A.; and McHugh, F. J.: Recent Advances in Rotor Technology at Boeing Vertol. 38th Annual Forum of the American Helicopter Society, Anaheim, Calif., May 4-7, 1982, pp. 24-33.
5. Philippe, J. J.; and Vuillet, A.: Aerodynamic Design of Advanced Rotors with New Tip Shapes. 39th Annual Forum of the American Helicopter Society, St. Louis, Mo., May 9-11, 1983. Paper no. 1983-119, pp. 58-71.
6. Tauber, M. E.: Computerized Aerodynamic Design of a Low Transonic Noise Blade. NASA TM-85928, 1984.
7. Monnerie, Bernard; and Philippe, Jean-Jacques: Aerodynamic Problems of Helicopter Blade Tips. *Vertica*, vol. 2, no. 3/4, 1978, pp. 217-231.
8. Cardonna, Francis X.; and Isom, Morris P.: Subsonic and Transonic Potential Flow Over Helicopter Rotor Blades. *AIAA J.*, vol. 10, no. 12, Dec. 1972, pp. 1606-1612.
9. Cardonna, Francis X.; and Isom, Morris P.: Numerical Calculation of Unsteady Transonic Potential Flow Over Helicopter Rotor Blades. *AIAA J.*, vol. 14, no. 4, Apr. 1976, pp. 482-488.
10. Grant, J.: Calculation of the Supercritical Flow Over the Tip Region of a Non-Lifting Rotor Blade at Arbitrary Azimuth. Royal Aircraft Establishment Technical Report 77180, Dec. 1977.
11. Arieli, R.; and Tauber, M. E.: Computation of Subsonic and Transonic Flow about Lifting Rotor Blades. Atmospheric Flight Mechanics Conference for Future Space Systems, Boulder, Colo., Aug. 6-8, 1979. Paper no. 79-1667, pp. 314-323.

12. Arieli, R.; and Tauber, M. E.: Analysis of the Quasi-Steady Flow about an Isolated Lifting Helicopter Rotor Blade. Joint Institute for Aeronautics and Acoustics, TR-24, Stanford University, Stanford, Calif., Aug. 1979.
13. Tung, C.; Pucci, S. L.; Caradonna, F. X.; and Morse, H. A.: The Structure of Trailing Vortices Generated by Model Rotor Blades. NASA TM-81316, 1981.
14. Chattot, J. J.: Calculation of Three-Dimensional Unsteady Transonic Flows Past Helicopter Blades. NASA TP-1721, 1980.
15. Tauber, M. E.; Chang, I. C.; Caughey, D. A.; and Philippe, J. J.: Comparison of Calculated and Measured Pressures on Straight and Swept-Tip Model Rotor Blades. NASA TM-85872, 1983.
16. Huston, R. J. (comp.): Rotorcraft Noise, NASA CP-2234, 1982.
17. Schmitz, F. H.; and Yu, Y. H.: Transonic Rotor Noise-Theoretical and Experimental Comparisons. Sixth European Rotorcraft and Powered Lift Aircraft Forum. Bristol, England, Sept. 1980. AD-A090806.
18. Tauber, M. E.; Owen, F. K.; Langhi, R. C.; and Palmer, G. E.: Comparison of Calculated and Measured Velocities Near the Tip of a Model Rotor Blade at Transonic Speeds. NASA TM-86697, Aug. 1985.
19. Gill, P. E.; Murray, W.; and Wright, M. H.: Practical Optimization. Academic Press, London, England, 1981.
20. Kennelly, R. A., Jr.: Improved Method for Transonic Airfoil Design-by-Optimization, American Institute of Aeronautics and Astronautics, Applied Aerodynamics Conference, Danvers, MA, Jul. 13-15, 1983.
21. Hicks, R. M.; and McCroskey, W. J.: An Experimental Evaluation of a Helicopter Rotor Section Designed by Numerical Optimization. NASA TM-78622, 1980.
22. Collins, Leslie; and Saunders, David: PROFILE User's Guide. NASA CR-177332, Feb. 1985 (Informatics General Corp.; NASA Contract NAS 2-11555).
23. Tauber, Michael E.; and Hicks, Raymond M.: Computerized Three-Dimensional Aerodynamic Design of a Lifting Rotor Blade. 36th Annual Forum of the American Helicopter Society,, Washington, D.C., May 1980. Paper 80-2, pp. 80-2-1 to 80-2-11.
24. Ramamoorthy, P.; and Padmavathi, K.: Airfoil Design by Optimization. J. of Aircraft, vol. 14, no. 2, Feb. 1977, pp. 219-221.



TABLE 1.- FORCE AND MOMENT COEFFICIENTS FOR  
UNMODIFIED RECTANGULAR BLADE

$\psi$ , deg	$\theta_c$ deg	$C_T$	$C_Q$	$C_M$
60	1.0	$5.251 \times 10^{-3}$	$9.280 \times 10^{-5}$	$-1.504 \times 10^{-4}$
75	-.1	$4.677 \times 10^{-3}$	$5.547 \times 10^{-5}$	$-2.084 \times 10^{-4}$
90	-.5	$4.328 \times 10^{-3}$	$3.751 \times 10^{-5}$	$-2.307 \times 10^{-4}$
105	-.1	$4.833 \times 10^{-3}$	$4.758 \times 10^{-5}$	$-2.128 \times 10^{-4}$
120	1.0	$5.629 \times 10^{-3}$	$8.106 \times 10^{-5}$	$-1.677 \times 10^{-4}$

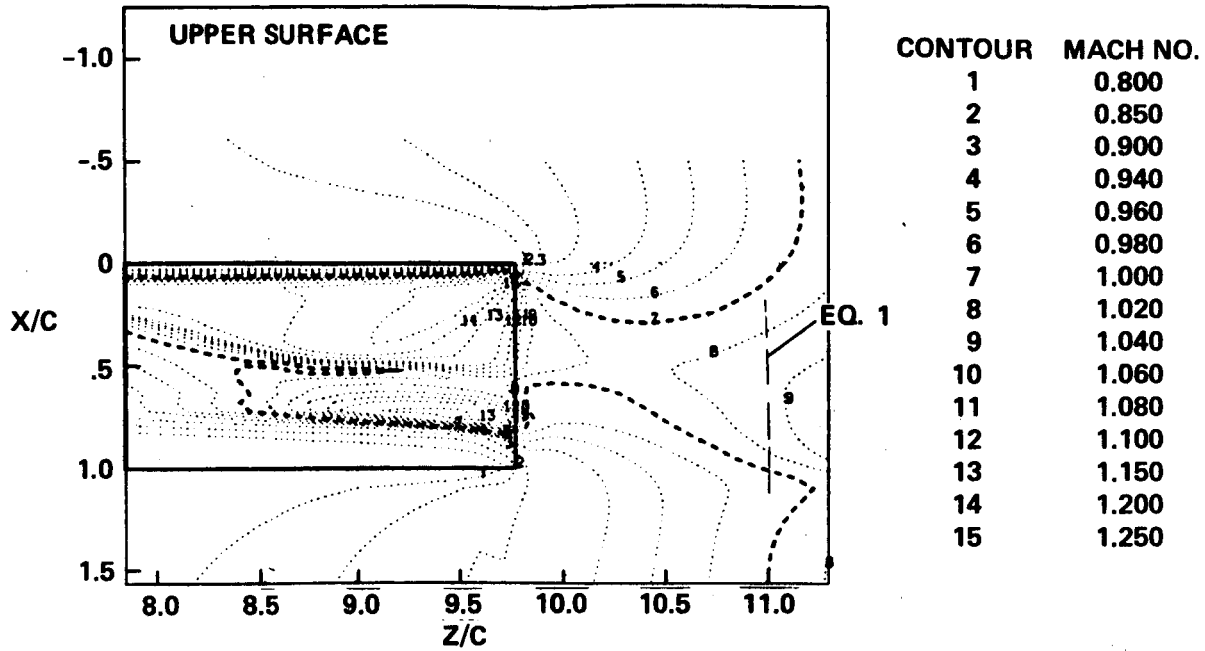


Figure 1.- Mach contours on rectangular tip with NLR-1 airfoil section,  $\psi = 90^\circ$ .

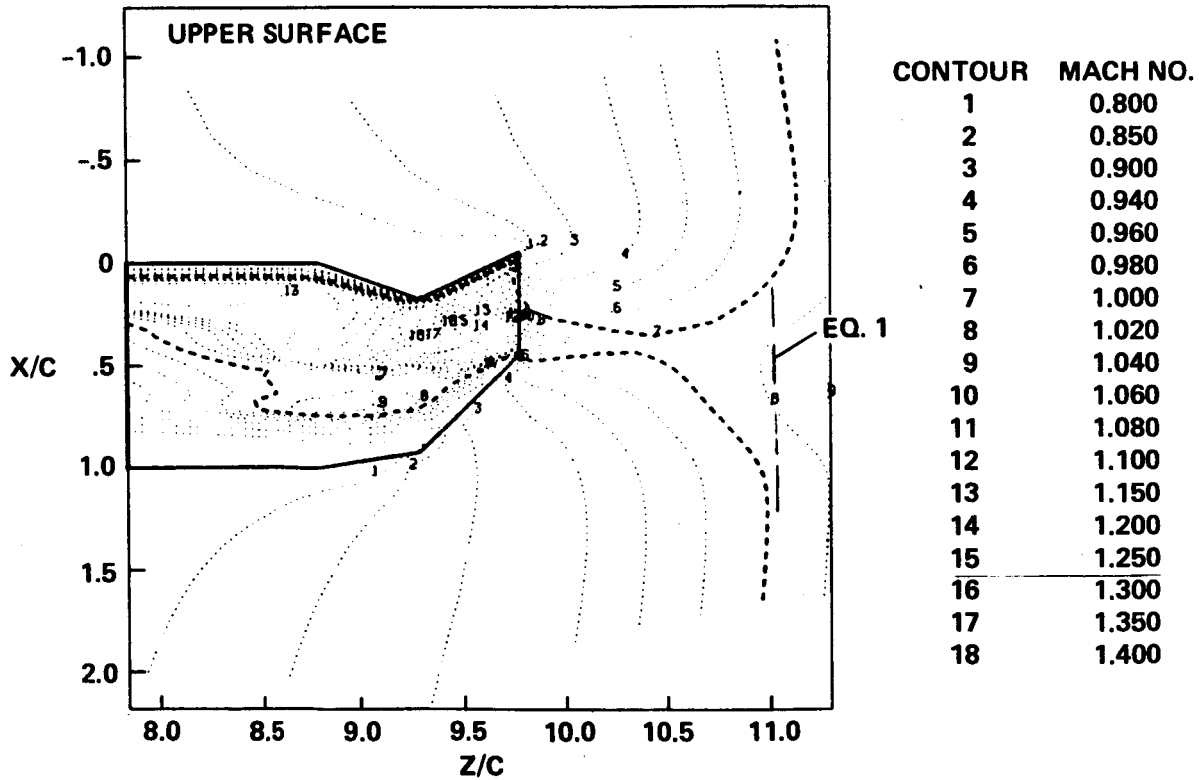


Figure 2.- Mach contours on  $20^\circ/-25^\circ$  swept tip with NLR-1 airfoil section,  $\psi = 90^\circ$ .

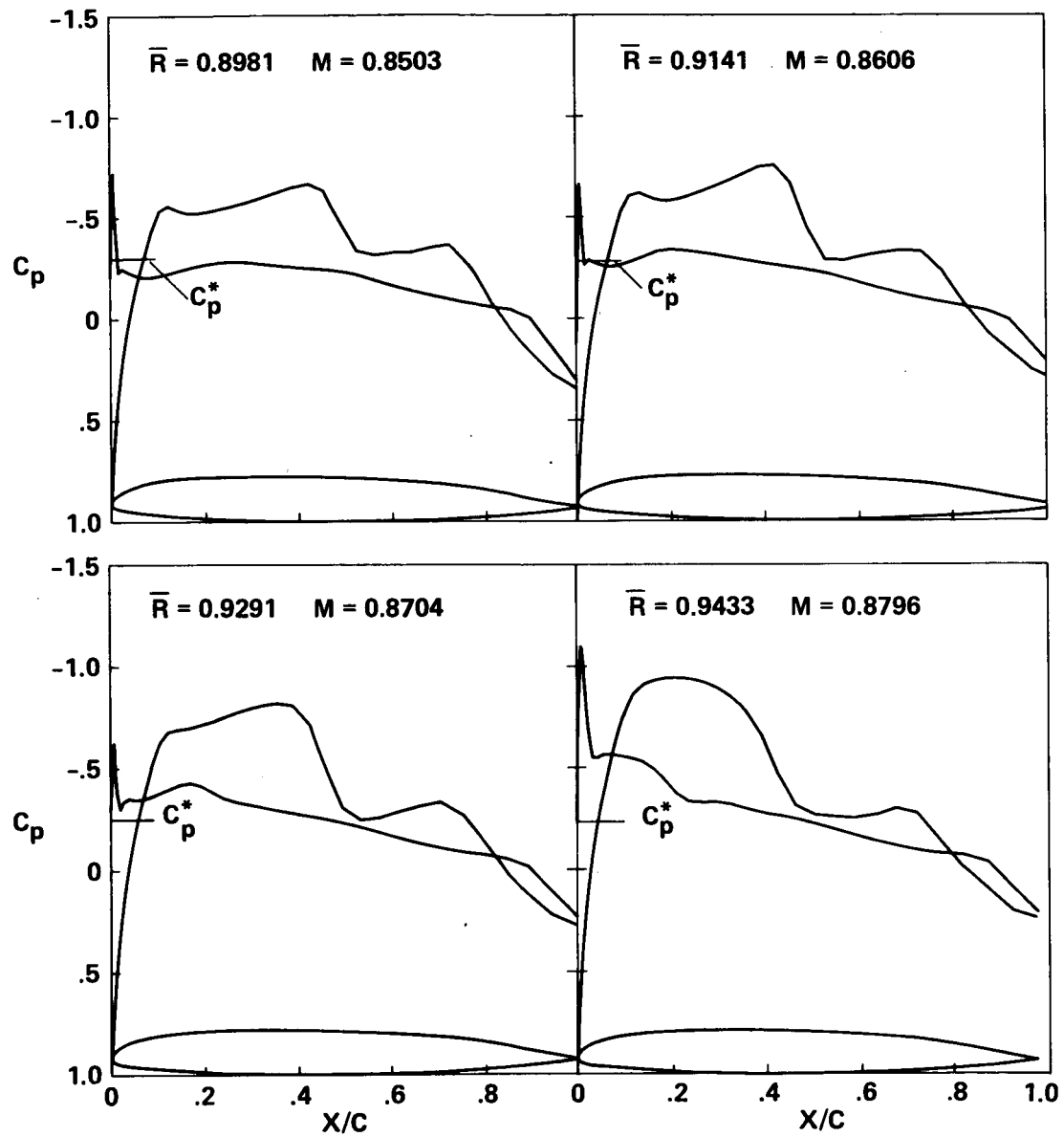


Figure 3.- Pressures on unmodified NLR-1 airfoil sections; sweep  $20^\circ/-25^\circ$ ,  $\psi = 90^\circ$ .

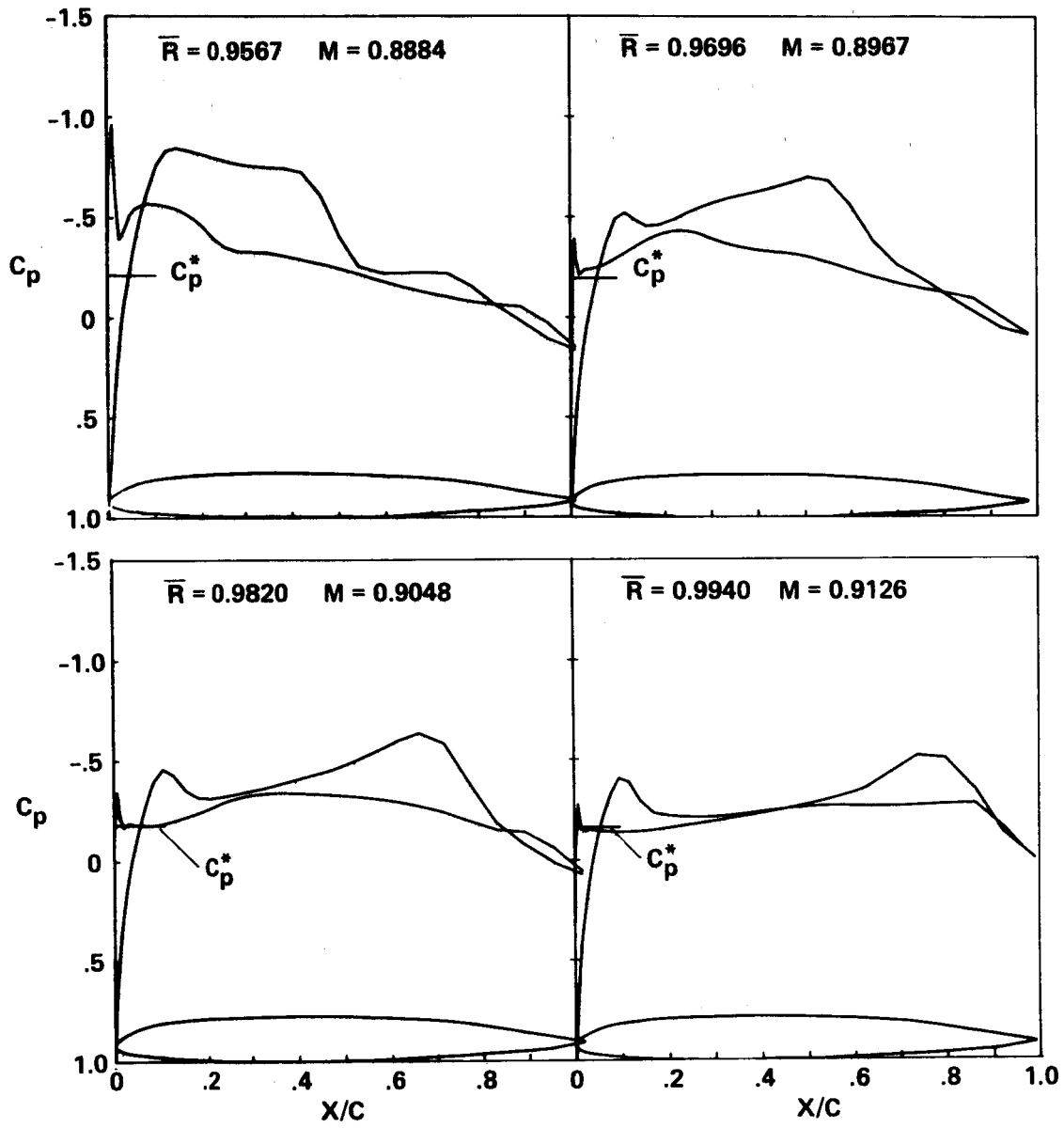


Figure 3.- Concluded.

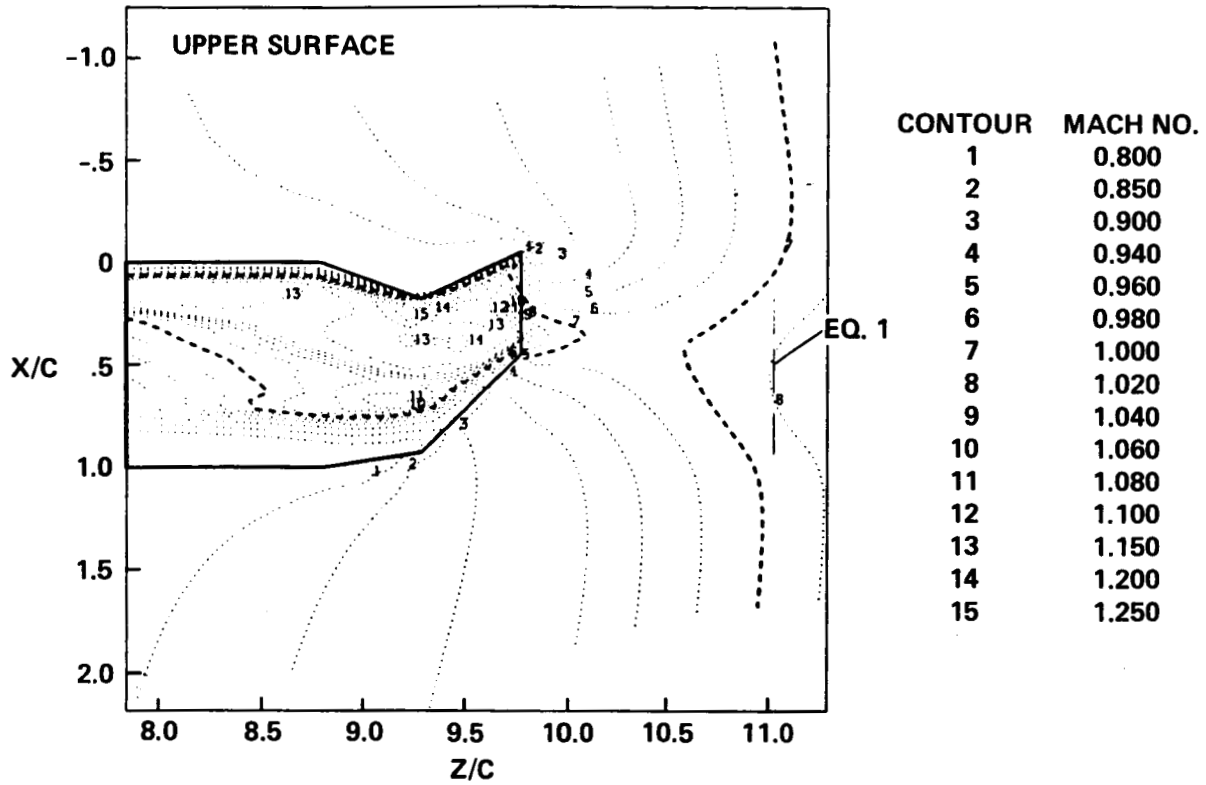


Figure 4.- Mach contours on 20°/-25° swept tip with "hand-modified" airfoil sections,  $\psi = 90^\circ$ .

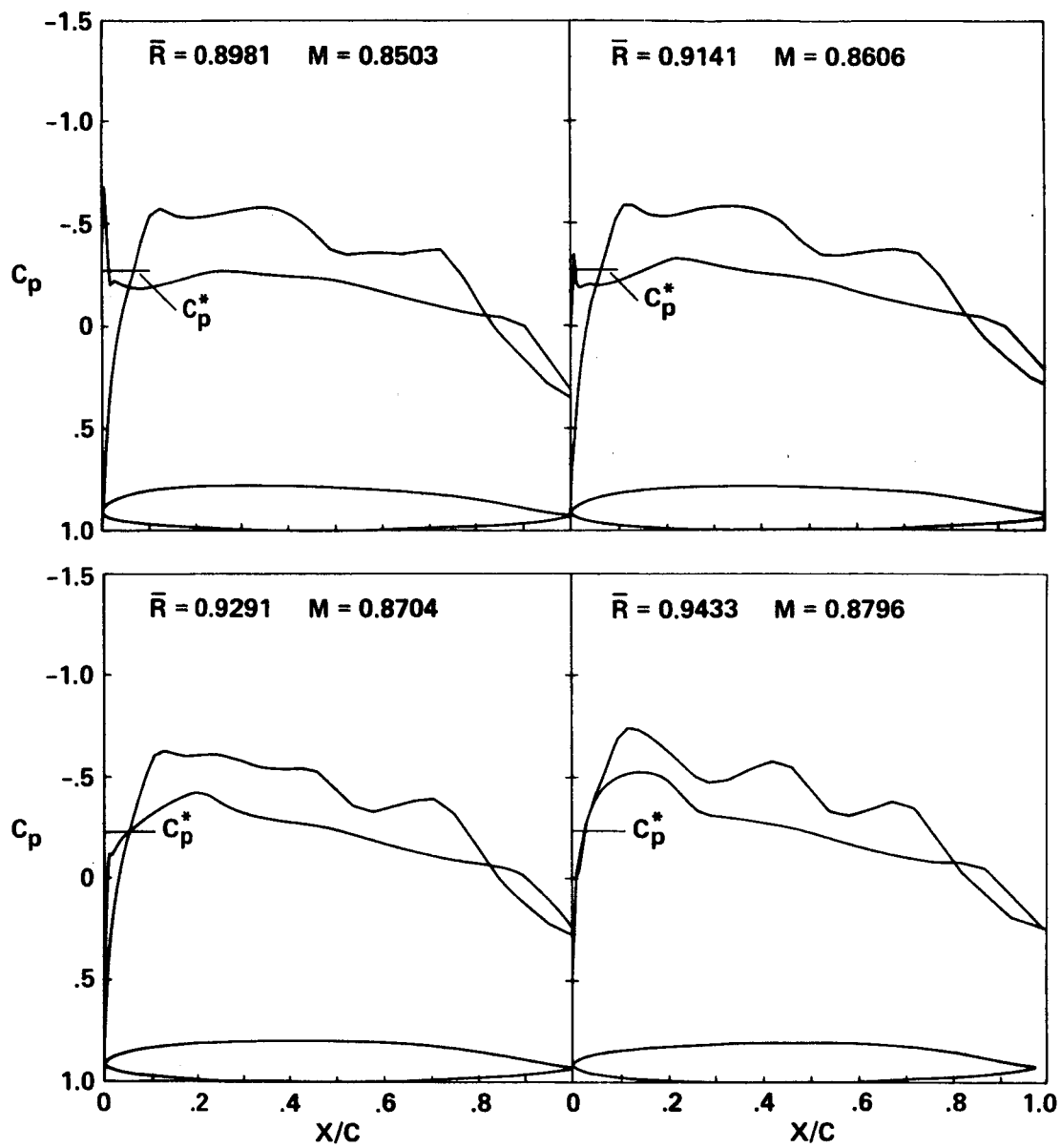


Figure 5.- Pressures on "hand-modified" airfoil sections; sweep  $20^\circ/-25^\circ$ ,  $\psi = 90^\circ$ .

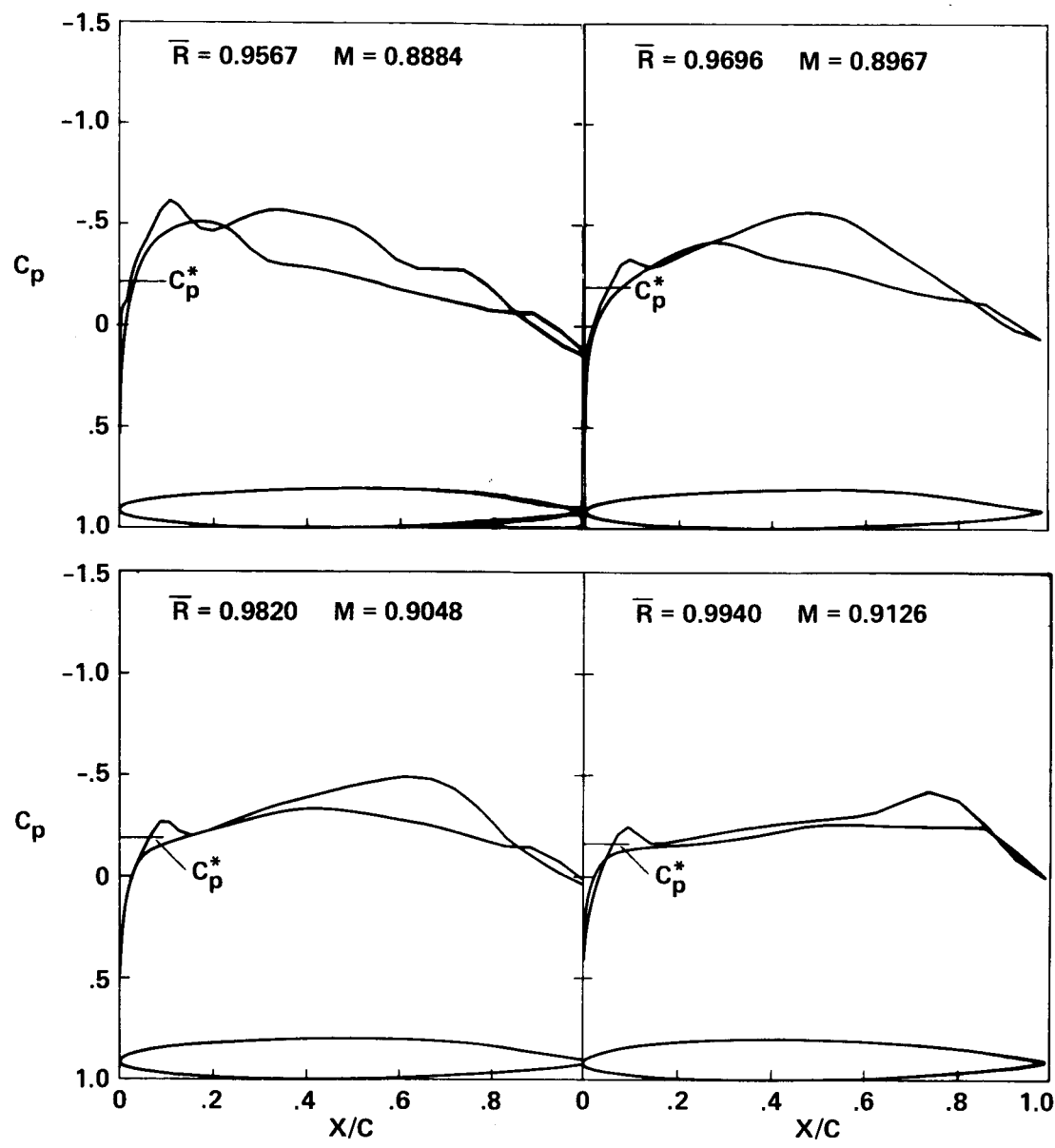


Figure 5.- Concluded.

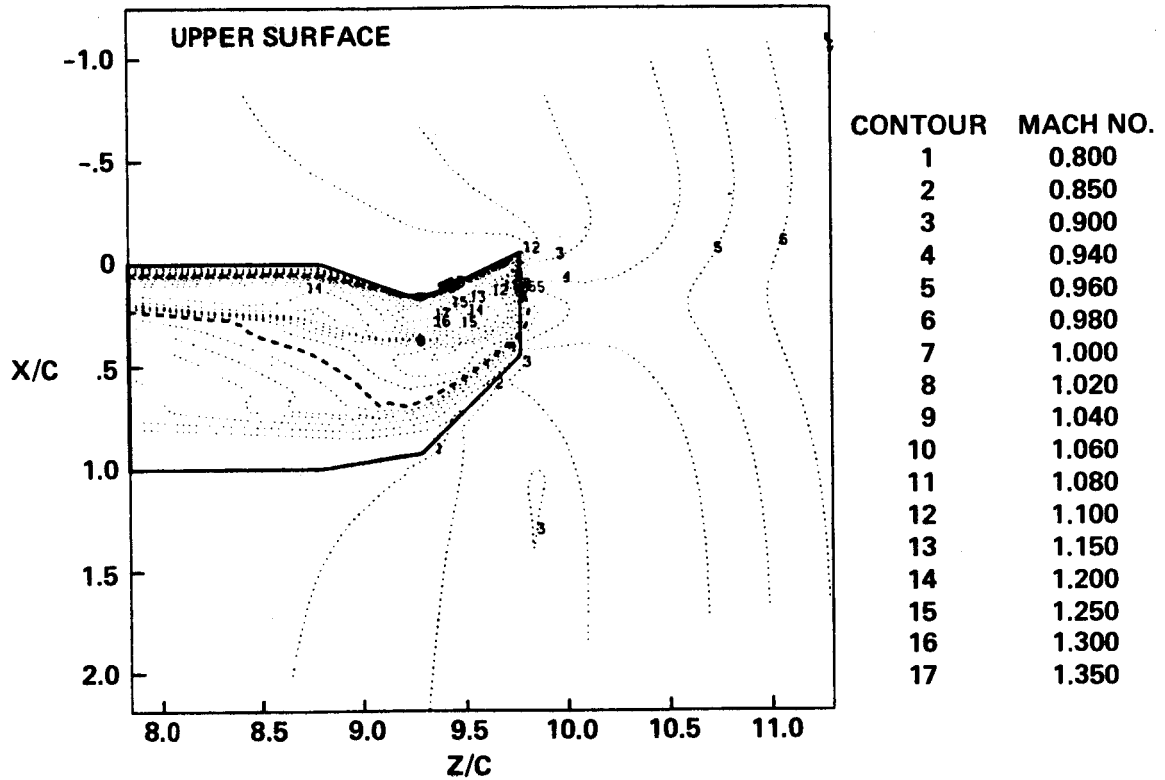


Figure 6.- Mach contours on 20°/-25° swept tip with "hand-modified" airfoil sections,  $\psi = 60^\circ$ .



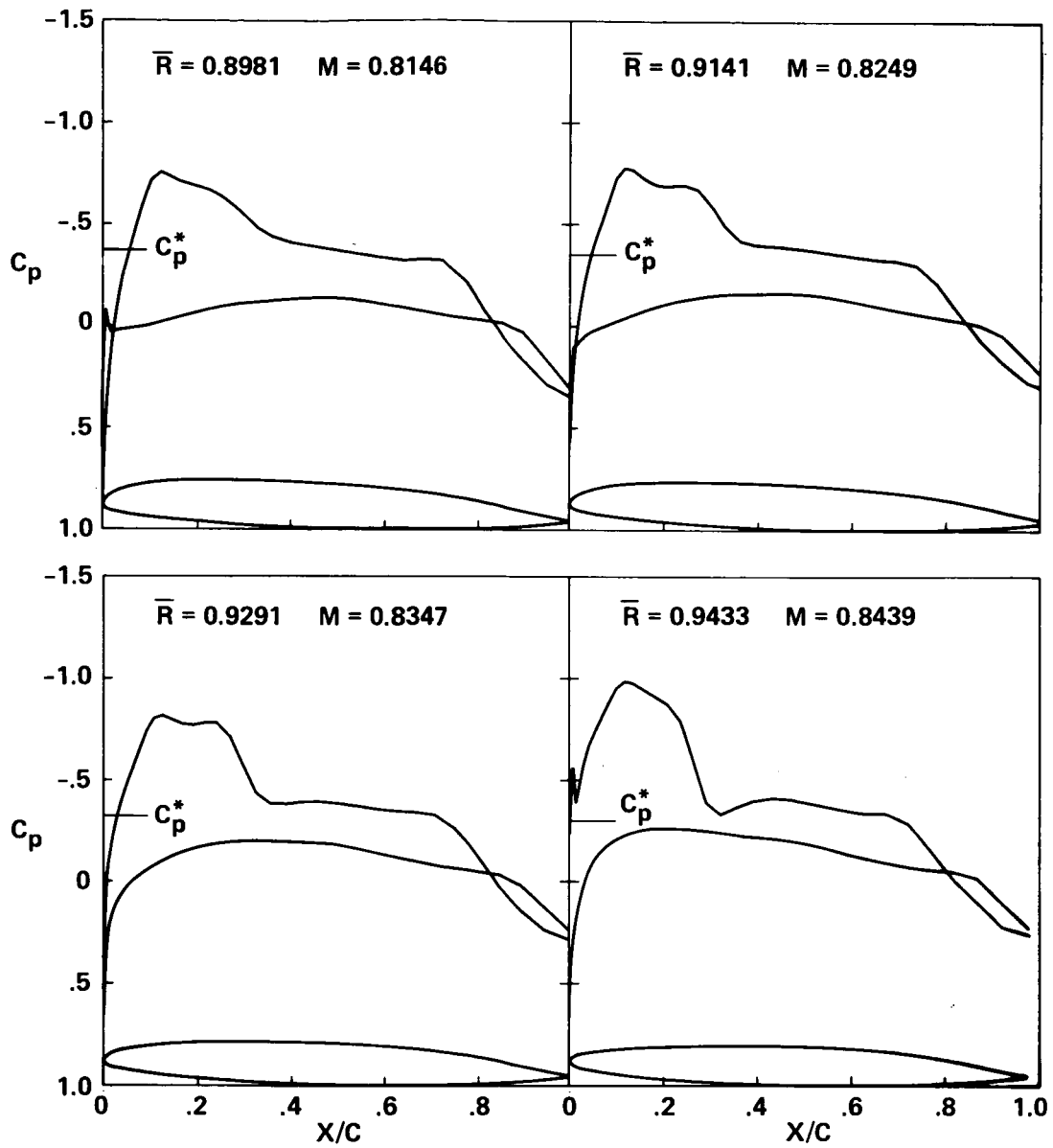


Figure 7.- Pressures on "hand-modified" airfoil sections; sweep  $20^\circ/-25^\circ$ ,  $\psi = 60^\circ$ .

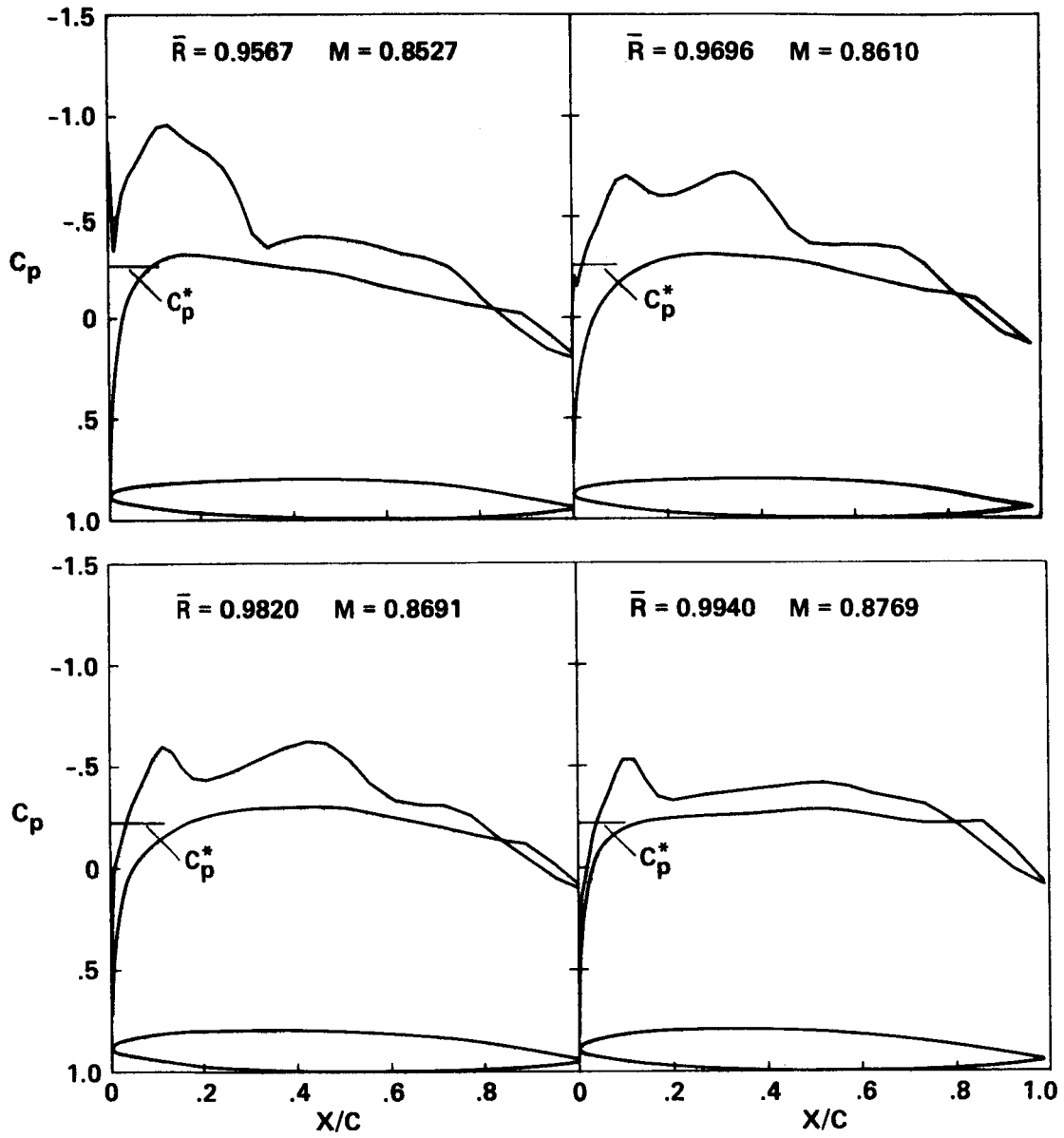


Figure 7.- Concluded.

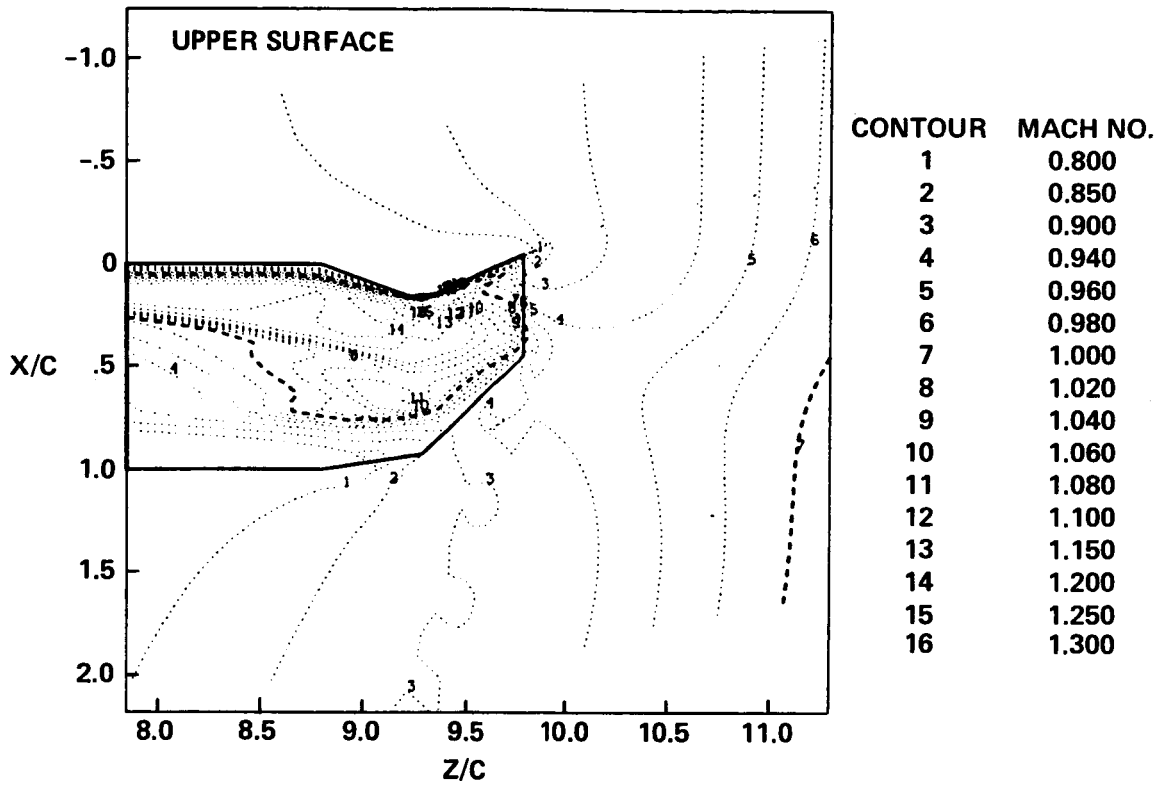


Figure 8.- Mach contours on 20°/-25° swept tip with "hand-modified" airfoil sections,  $\psi = 120^\circ$ .

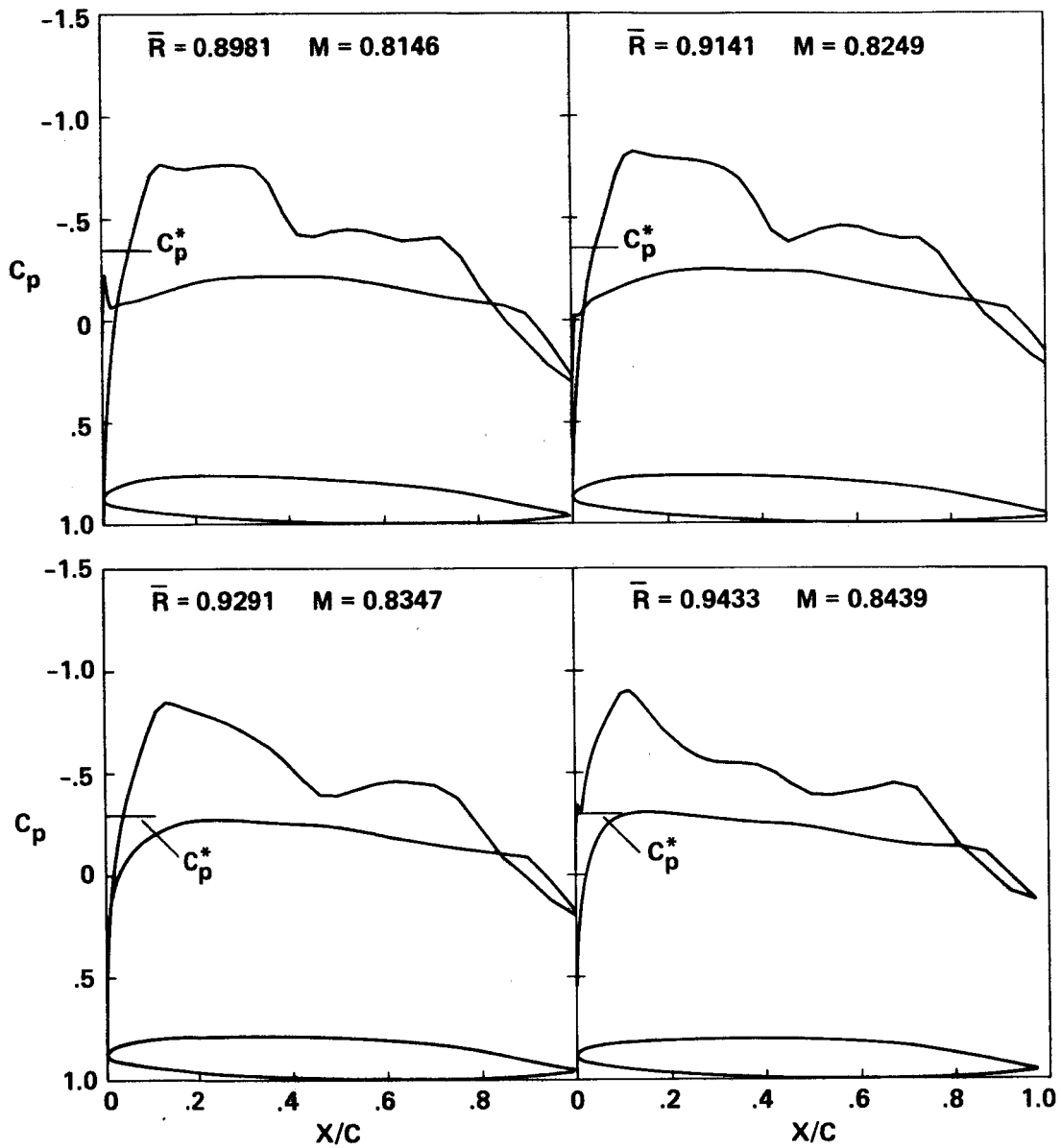


Figure 9.- Pressures on "hand-modified" airfoil sections; sweep  $20^\circ/-25^\circ$ ,  $\psi = 120^\circ$ .

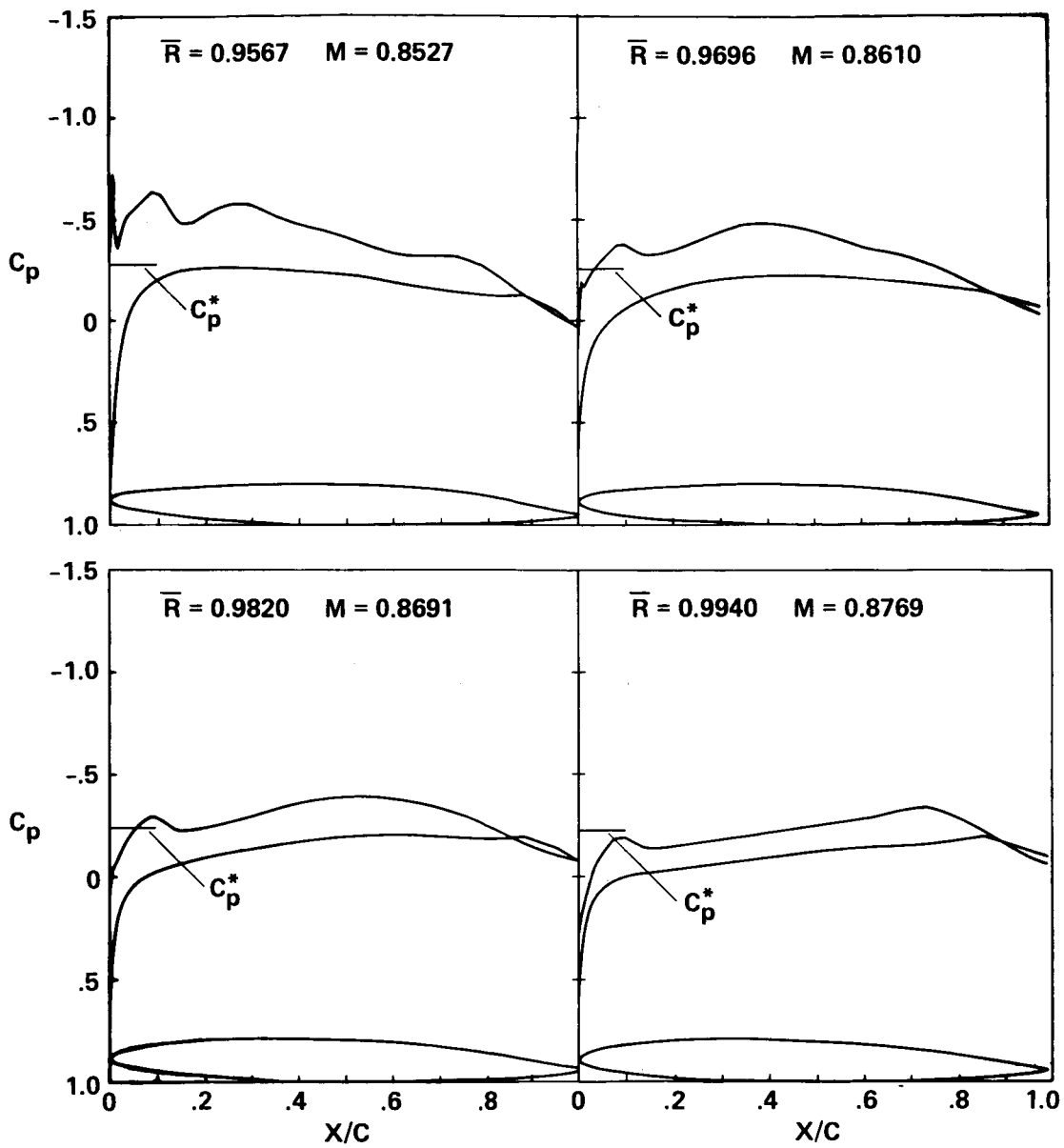


Figure 9.- Concluded.

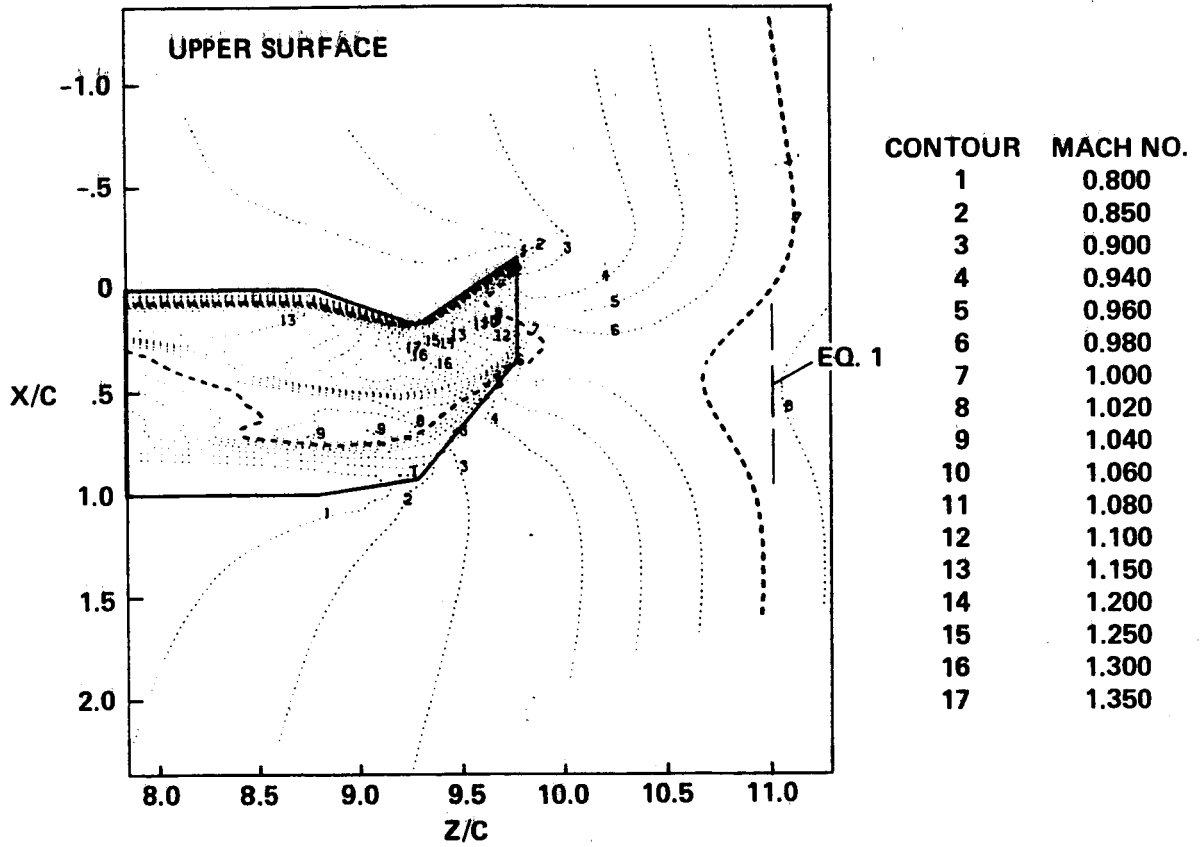


Figure 10.- Mach contours on optimized tip, sweep  $19.7^\circ/-34.1^\circ$ ,  $\psi = 90^\circ$ .

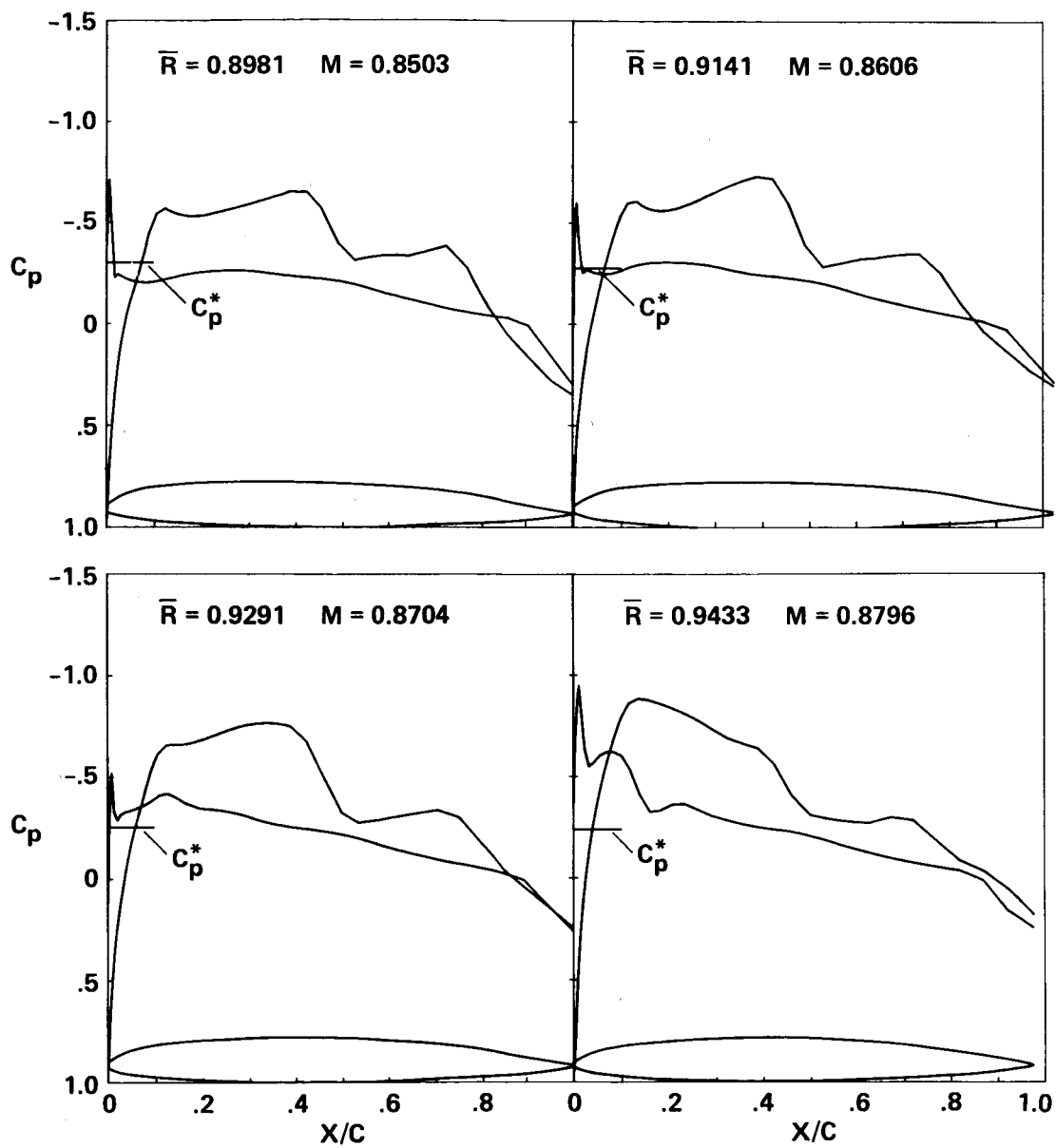


Figure 11.- Pressures on optimized tip; sweep  $19.7^\circ/-34.1^\circ$ ,  $\psi = 90^\circ$ .

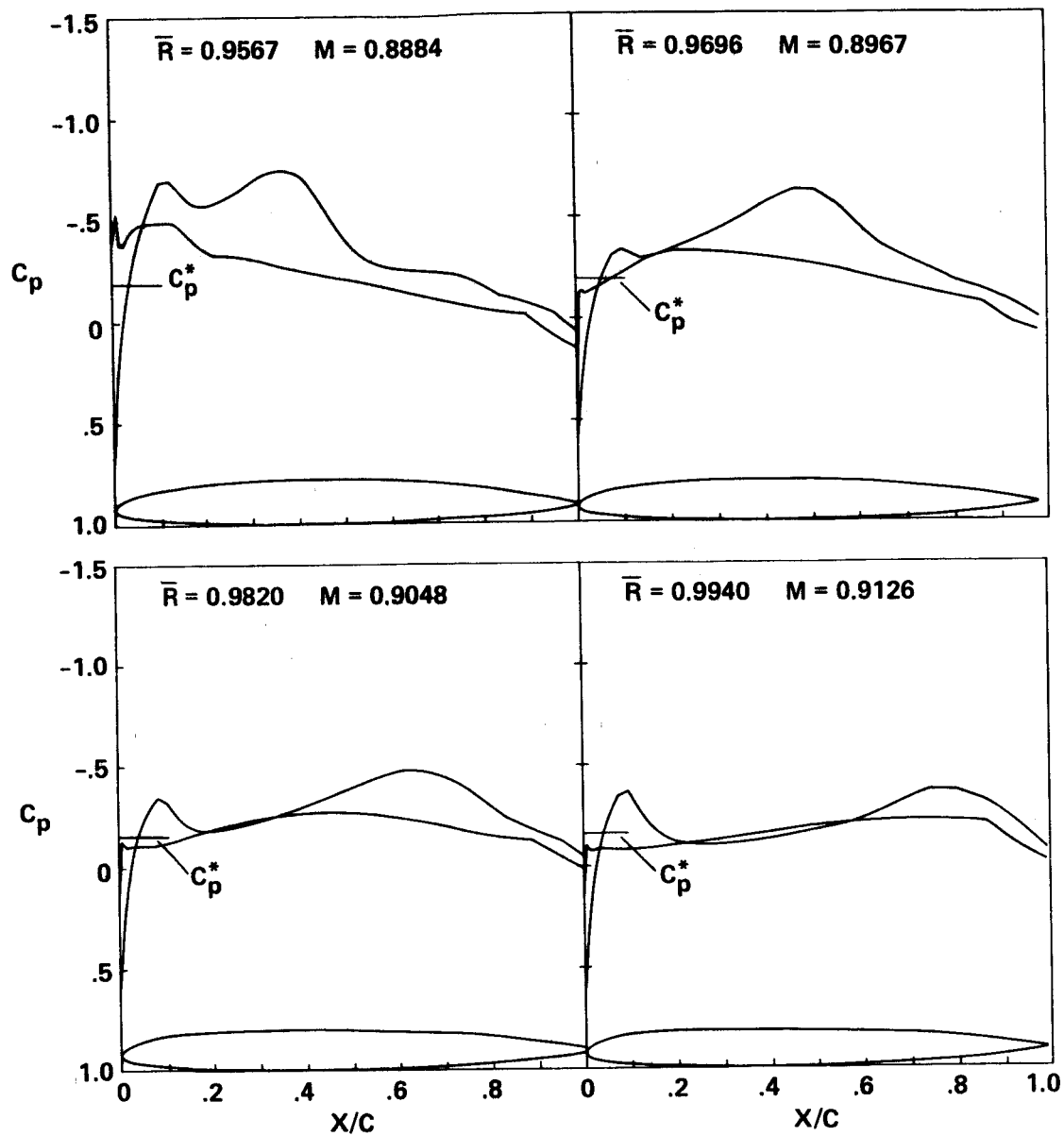


Figure 11.- Concluded.



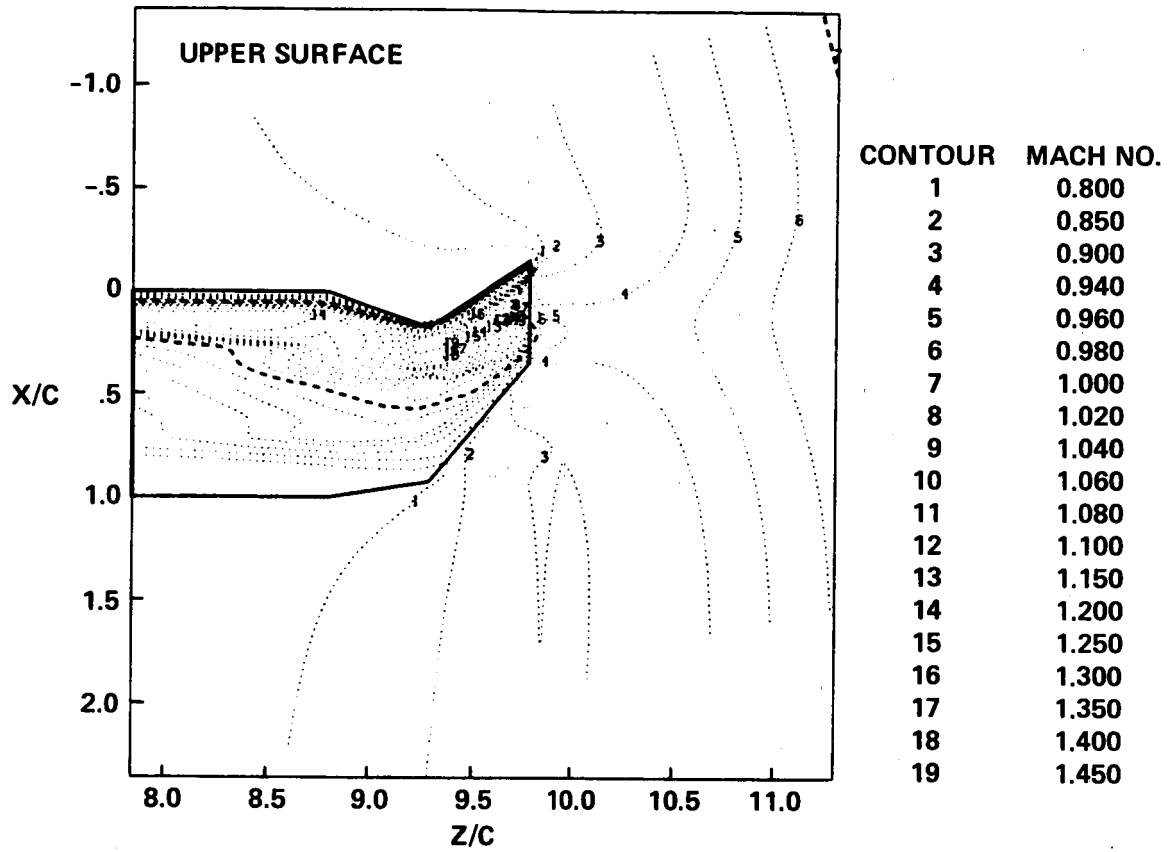


Figure 12.- Mach contours on optimized tip, sweep  $19.7^\circ/-34.1^\circ$ ,  $\psi = 60^\circ$ .

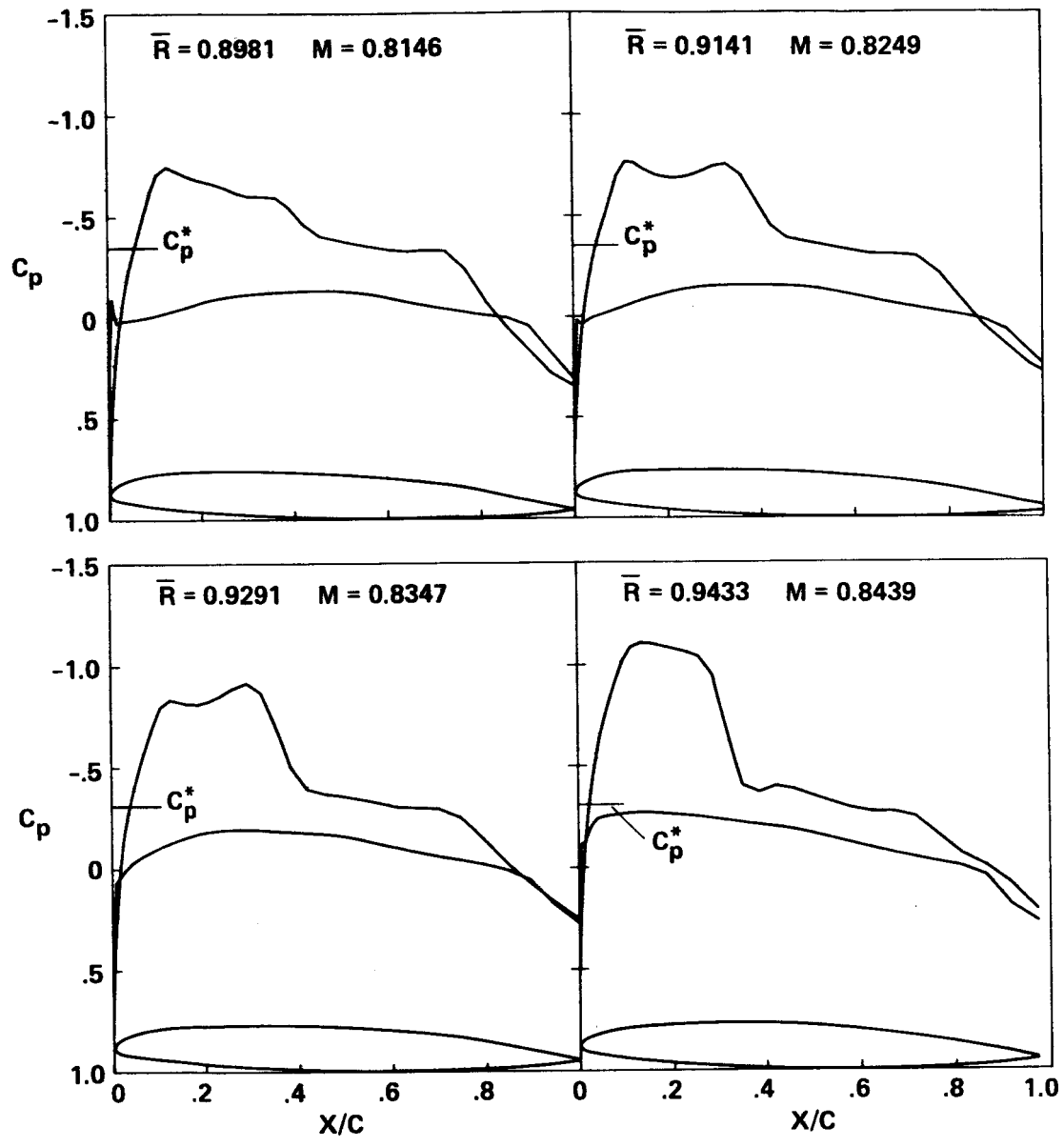


Figure 13.- Pressures on optimized tip; sweep  $19.7^\circ/-34.1^\circ$ ,  $\psi = 60^\circ$ .

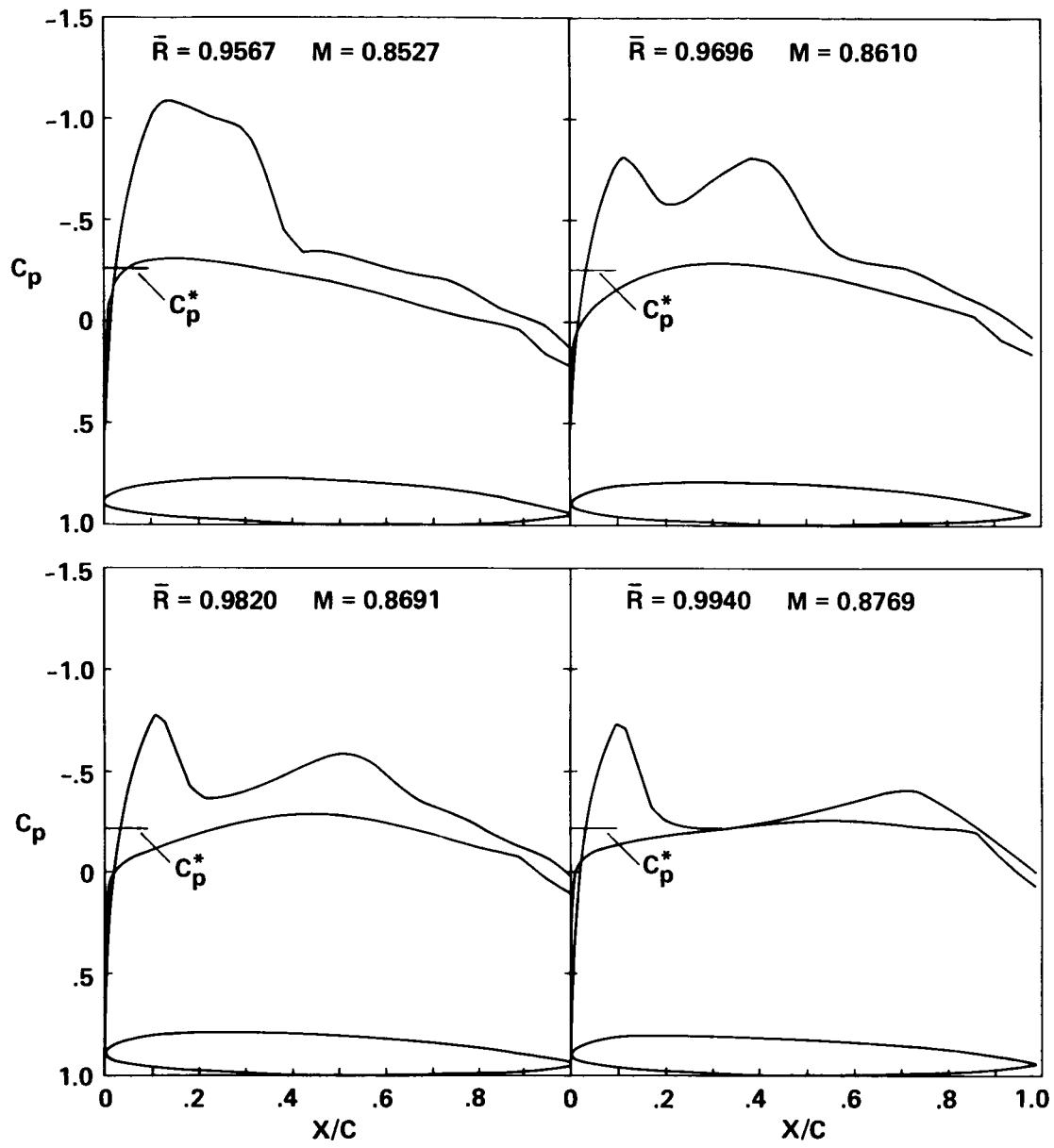


Figure 13.- Concluded.

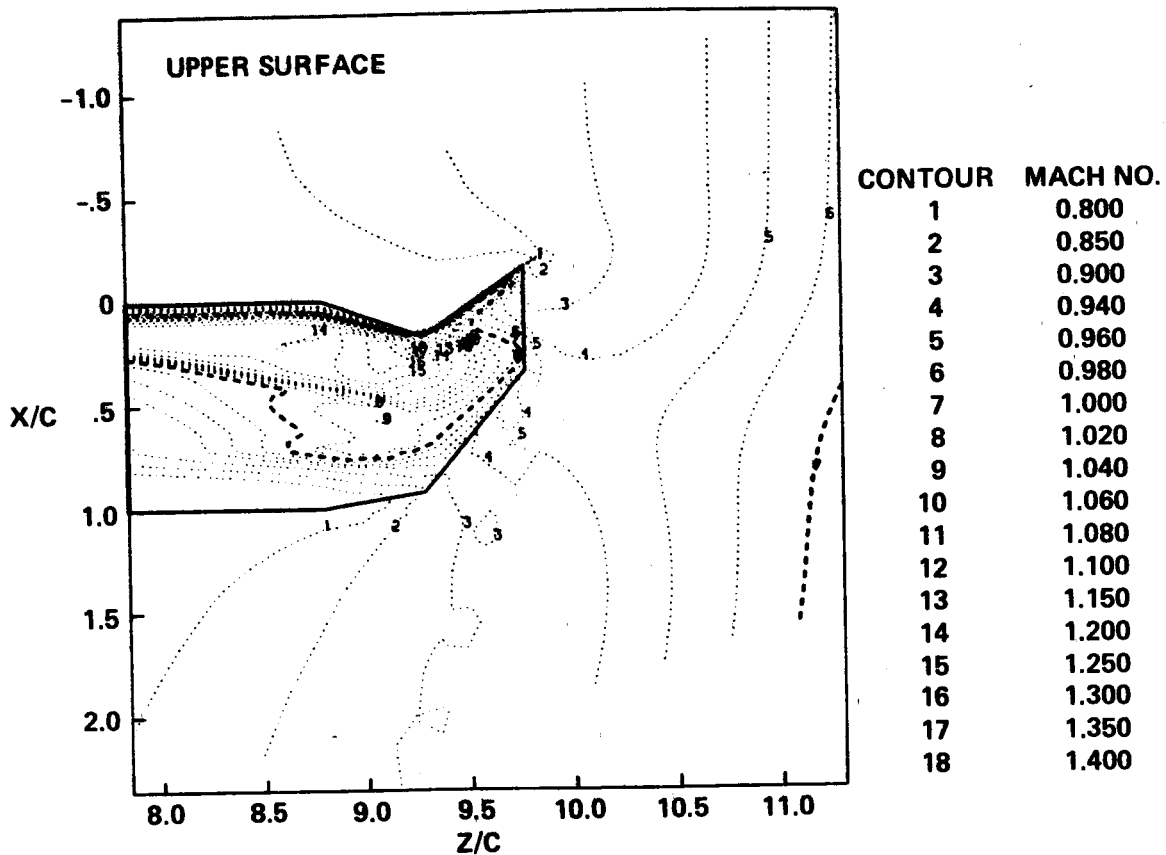


Figure 14.- Mach contours on optimized tip, sweep  $19.7^\circ/-34.1^\circ$ ,  $\psi = 120^\circ$ .

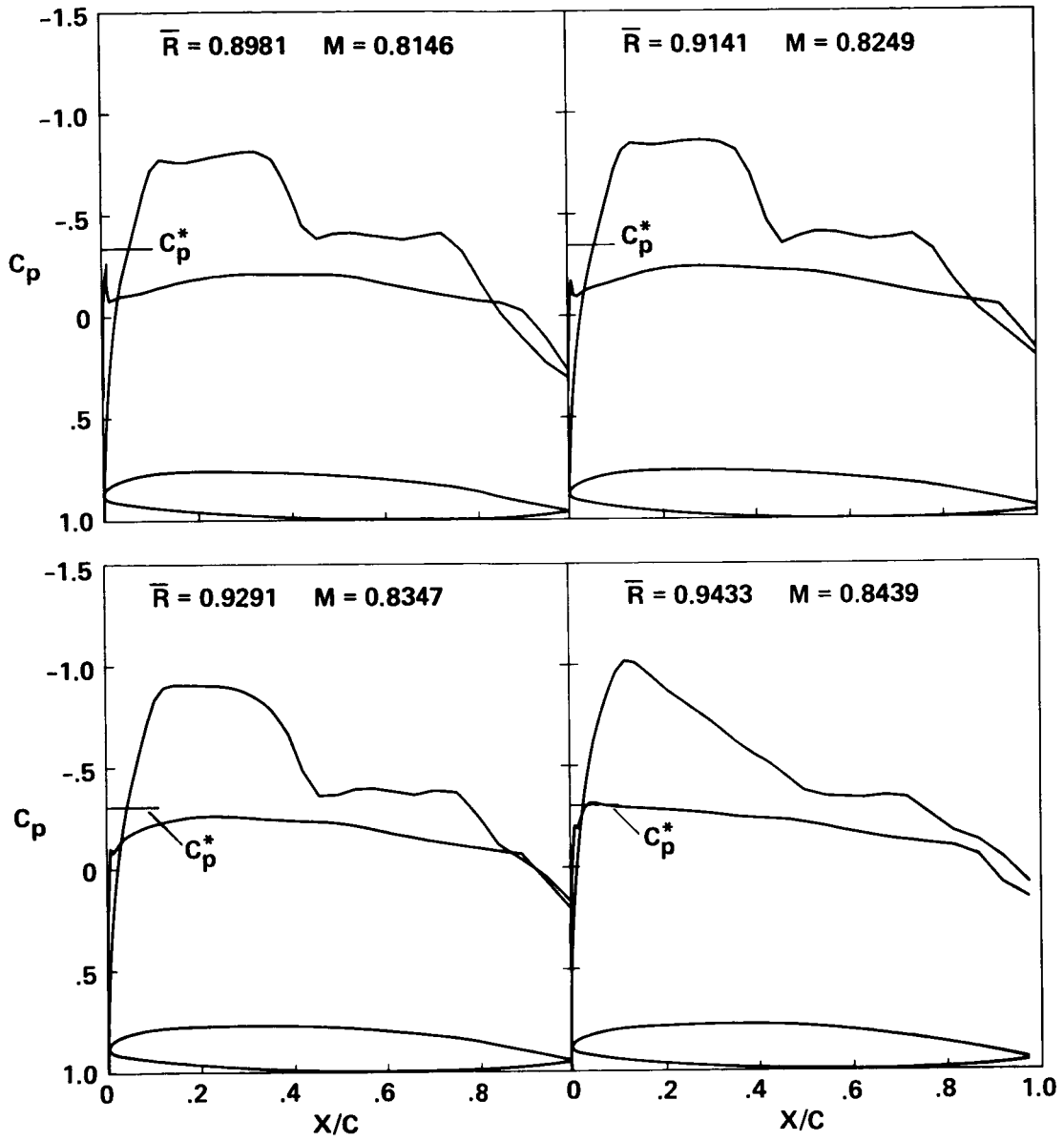


Figure 15.- Pressures on optimized tip; sweep  $19.7^\circ/-34.1^\circ$ ,  $\psi = 120^\circ$ .

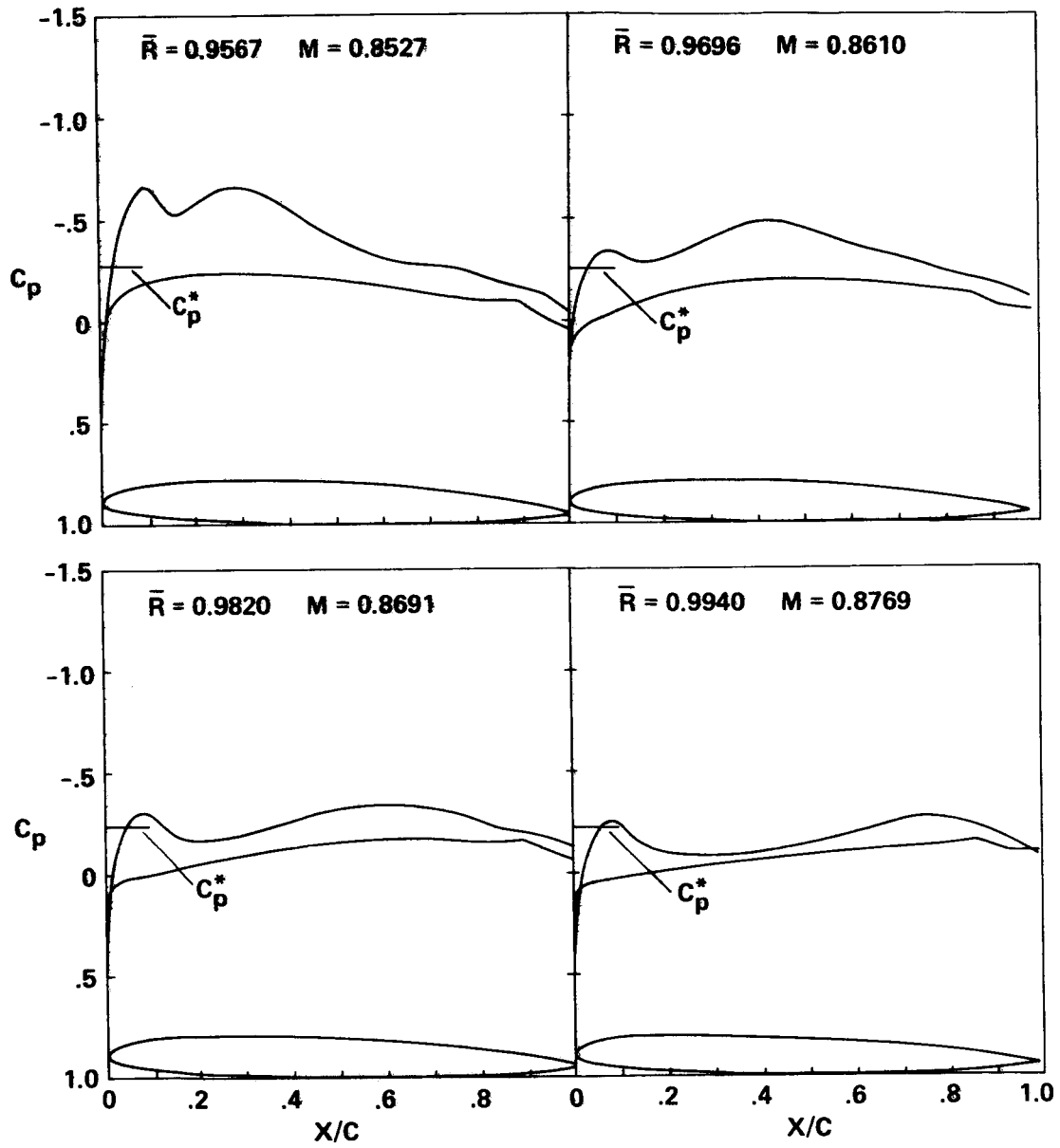


Figure 15.- Concluded.

- UNMODIFIED SECTIONS, PLANFORM 30 deg SWEEP BACK
- HAND-MODIFIED SECTIONS, PLANFORM ANGLES 20/-25 deg
- △ OPTIMIZED SECTIONS, PLANFORM ANGLES 19.7/-34.1 deg
- + UNMODIFIED SECTIONS, PLANFORM 20 deg SWEEP FORWARD

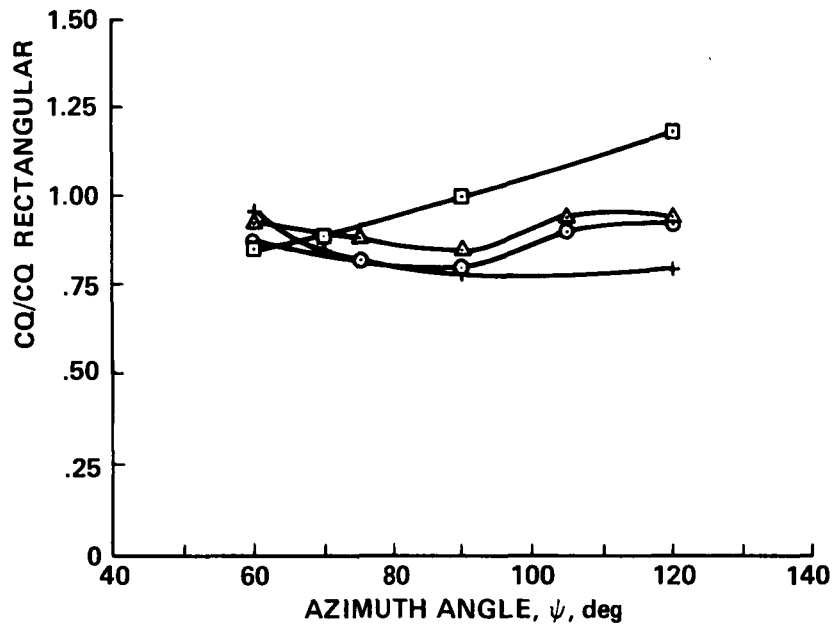


Figure 16.- Normalized torque comparison for blades with four modified tips.

- UNMODIFIED SECTIONS, PLANFORM 30 deg SWEPT BACK
- HAND-MODIFIED SECTIONS, PLANFORM ANGLES 20/-25 deg
- △ OPTIMIZED SECTIONS, PLANFORM ANGLES 19.7/-34.1 deg
- + UNMODIFIED SECTIONS, PLANFORM 20 deg SWEPT FORWARD

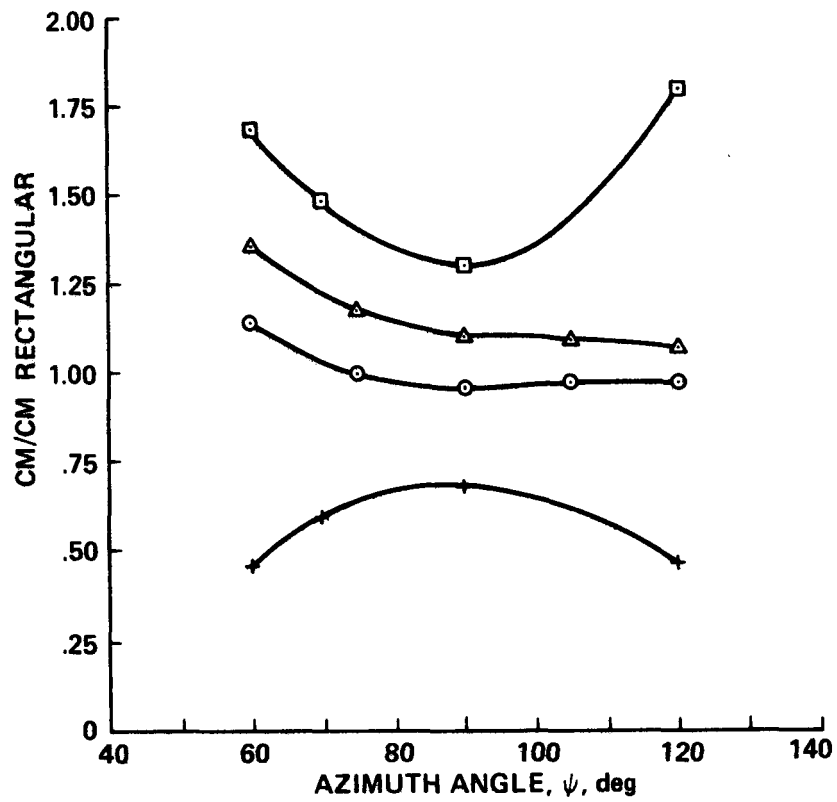



Figure 17.- Normalized pitching moment comparison for blades with four modified tips.



1. Report No. NASA TM-86771		2. Government Accession No.		3. Recipient's Catalog No.	
4. Title and Subtitle TRANSONIC ROTOR TIP DESIGN USING NUMERICAL OPTIMIZATION				5. Report Date September 1985	
				6. Performing Organization Code	
7. Author(s) Michael E. Tauber and Ronald G. Langhi				8. Performing Organization Report No. 85333	
9. Performing Organization Name and Address  Ames Research Center Moffett Field, CA 94035				10. Work Unit No.	
				11. Contract or Grant No.	
12. Sponsoring Agency Name and Address  National Aeronautics and Space Administration Washington, DC 20546				13. Type of Report and Period Covered  Technical Memorandum	
				14. Sponsoring Agency Code  505-42-11	
15. Supplementary Notes  Point of Contact: Michael E. Tauber, Ames Research Center, MS 229-4, Moffett Field, CA 94035 (415)694-5372 or FTS 464-5372					
16. Abstract  The aerodynamic design procedure for a new blade tip suitable for operation at transonic speeds is illustrated. For the first time, three-dimensional numerical optimization was applied to rotor tip design, using the recent derivative of the ROT22 code, program R22OPT. Program R22OPT utilized an efficient quasi-Newton optimization algorithm. Multiple design objectives were specified. The delocalization of the shock wave was to be eliminated in forward flight for an advance ratio of 0.41 and a tip Mach number of 0.92 at $\psi = 90^\circ$ . Simultaneously, it was sought to reduce torque requirements while maintaining effective restoring pitching moments. Only the outer 10% of the blade span was modified; the blade area was not to be reduced by more than 3%. The goal was to combine the advantages of both swept-back and swept-forward blade tips (configurations which had been studied previously). A planform that featured inboard sweepback was combined with a swept-forward tip and a taper ratio of 0.5. Initially, the ROT22 code was used to find by trial and error a planform geometry which met the design goals. This configuration had an inboard section with a leading edge sweep of $20^\circ$ and a tip section swept forward at $25^\circ$ ; in addition, the airfoils were modified. With this tip shape as a starting point, program R22OPT was used to improve the planform and airfoil section design. Significant improvements, which met all design objectives, were achieved in 2.5 CPU hours on a CRAY X-MP computer. The optimized tip has an inboard sweepback of $19.7^\circ$ , a tip swept forward at $34.1^\circ$ , 50% of taper, and modified airfoil sections.					
17. Key Words (Suggested by Author(s))  Helicopter aerodynamics Numerical optimization			18. Distribution Statement    Subject Category - 02		
19. Security Classif. (of this report)  Unclassified		20. Security Classif. (of this page)  Unclassified		21. No. of Pages  41	22. Price*  A03